Journal of Virology

Identification of Alternative Transcripts Encoding the Essential Murine Gammaherpesvirus Lytic Transactivator RTA

Brian S. Wakeman, L. Steven Johnson, Clinton R. Paden, Kathleen S. Gray, Herbert W. Virgin and Samuel H. Speck

Updated information and services can be found at:
http://jvi.asm.org/content/88/10/5474

These include:

REFERENCES

This article cites 67 articles, 41 of which can be accessed free at: http://jvi.asm.org/content/88/10/5474#ref-list-1

CONTENT ALERTS

Receive: RSS Feeds, eTOCs, free email alerts (when new articles cite this article), more»

Journals.ASM.org

Identification of Alternative Transcripts Encoding the Essential Murine Gammaherpesvirus Lytic Transactivator RTA

Brian S. Wakeman,[a] L. Steven Johnson,[b] Clinton R. Paden,[a] Kathleen S. Gray,[a] Herbert W. Virgin,[b] Samuel H. Speck[a]

Emory Vaccine Center and Department of Microbiology & Immunology, Emory University School of Medicine, Atlanta, Georgia, USA[a]; Department of Pathology and Immunology, Washington University School of Medicine, St. Louis, Missouri, USA[b]

ABSTRACT

The essential immediate early transcriptional activator RTA, encoded by gene 50, is conserved among all characterized gammaherpesviruses. Analyses of a recombinant murine gammaherpesvirus 68 (MHV68) lacking both of the known gene 50 promoters (G50DblKo) revealed that this mutant retained the ability to replicate in the simian kidney epithelial cell line Vero but not in permissive murine fibroblasts following low-multiplicity infection. However, G50DblKo replication in permissive fibroblasts was partially rescued by high-multiplicity infection. In addition, replication of the G50DblKo virus was rescued by growth on mouse embryonic fibroblasts (MEFs) isolated from IFN-$\alpha/\beta R^{-/-}$ mice, while growth on Vero cells was suppressed by the addition of alpha interferon (IFN-α). 5′ rapid amplification of cDNA ends (RACE) analyses of RNAs prepared from G50DblKo and wild-type MHV68-infected murine macrophages identified three novel gene 50 transcripts initiating from 2 transcription initiation sites located upstream of the currently defined proximal and distal gene 50 promoters. In transient promoter assays, neither of the newly identified gene 50 promoters exhibited sensitivity to IFN-α treatment. Furthermore, in a single-step growth analysis RTA levels were higher at early times postinfection with the G50DblKo mutant than with wild-type virus but ultimately fell below the levels of RTA expressed by wild-type virus at later times in infection. Infection of mice with the MHV68 G50DblKo virus demonstrated that this mutant virus was able to establish latency in the spleen and peritoneal exudate cells (PECs) of C57BL/6 mice with about 1/10 the efficiency of wild-type virus or marker rescue virus. However, despite the ability to establish latency, the G50DblKo virus mutant was severely impaired in its ability to reactivate from either latently infected splenocytes or PECs. Consistent with the ability to rescue replication of the G50DblKo mutant by growth on type I interferon receptor null MEFs, infection of IFN-$\alpha/\beta R^{-/-}$ mice with the G50DblKo mutant virus demonstrated partial rescue of (i) acute virus replication in the lungs, (ii) establishment of latency, and (iii) reactivation from latency. The identification of additional gene 50/RTA transcripts highlights the complex mechanisms involved in controlling expression of RTA, likely reflecting time-dependent and/or cell-specific roles of different gene 50 promoters in controlling virus replication. Furthermore, the newly identified gene 50 transcripts may also act as negative regulators that modulate RTA expression.

IMPORTANCE

The viral transcription factor RTA, encoded by open reading frame 50 (Orf50), is well conserved among all known gammaherpesviruses and is essential for both virus replication and reactivation from latently infected cells. Previous studies have shown that regulation of gene 50 transcription is complex. The studies reported here describe the presence of additional alternatively initiated, spliced transcripts that encode RTA. Understanding how expression of this essential viral gene product is regulated may identify new strategies for interfering with infection in the setting of gammaherpesvirus-induced diseases.

Herpesviruses are large double-stranded DNA viruses. The hallmark of all herpesvirus infections is their ability to persist latently for the lifetime of the host, which is marked by sporadic virus reactivation, replication, and shedding. The herpesvirus family is divided into three classes, the alpha-, beta-, and gammaherpesviruses. While both alpha- and betaherpesviruses generally exhibit broad tropism and the ability to infect a range of cell types, gammaherpesviruses are unique in that they are mainly lymphotropic, infecting and establishing latency in T or B lymphocytes. Gammaherpesviruses are also unique in that they are associated with a variety of lymphomas. Kaposi's sarcoma-associated virus (KSHV) is associated with tumor development in its namesake Kaposi's sarcoma, as well as multicentric Castleman's disease and primary effusion lymphoma. Epstein-Barr virus (EBV) is tightly associated with the development of several human malignancies, including nasopharyngeal carcinoma, Hodgkin's lymphoma, Burkitt's lymphoma, and posttransplant lymphoproliferative disease (1). Though both KSHV- and EBV-associated malignancies are rare, their prevalence is elevated in people who are immunocompromised via either immunosuppressive therapies or HIV infection (2–4).

While in vitro cell culture systems exist to study the two human gammaherpesviruses EBV and KSHV, these viruses have a narrow host tropism which severely limits in vivo studies. This has generated a need for robust small-animal models to further investigate primary viral infection, establishment of latency, and reactivation in the context of natural infection. Murine gammaherpesvirus 68
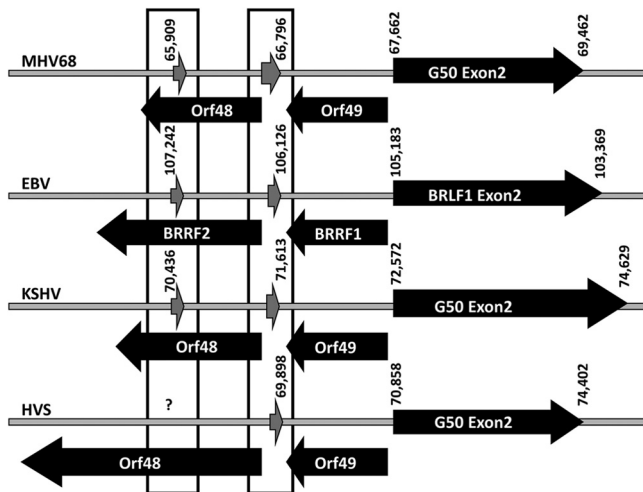
FIG 1 Genomic alignment of Orf50/BRLF1/Rta regions from MHV68, EBV, KSHV, and HVS gammaherpesviruses, illustrating the conserved organization of gene 50 transcription. A schematic diagram of the Orf50 region with exon 2, exon 1, and recently discovered exon 0 is shown. The antisense coding regions Orf48/BRRF2 and Orf49/BRRF1 are shown to demonstrate the conserved organizational context. The boxes around exon 1 and exon 0 shown their relative positions within the genome. The nucleotide positions of exon 0 (E0), exon 1 (E1), and exon 2 (E2) are given.

(MHV68) has emerged as the leading animal model for characterizing gammaherpesvirus pathogenesis *in vivo*. MHV68 is a natural pathogen of wild murid rodents and readily infects laboratory strains of mice (5). Complete sequencing of the MHV68 genome revealed extensive homology to those of both EBV and KSHV (6). MHV68 infects multiple organs, establishes latency in the spleen and lymph nodes, is primarily lymphotropic, and is associated with development of lymphoproliferative disease and lymphomas (7–9).

An area of the MHV68 genome that is well conserved in both sequence homology and function is the gene 50 region, which encodes the essential immediate early viral transcriptional activator RTA (also known as R or BRLF1). Notably, the MHV68, KSHV, and EBV gene 50 transcripts exhibit similar splicing patterns, promoters, and genome locations (Fig. 1). Furthermore, ectopic expression of RTA in cells latently infected with MHV68, herpesvirus saimiri (HVS), KSHV, and EBV is capable of driving virus reactivation (10, 11), mediated through RTA activation of viral lytic cycle-associated gene promoters (12, 13–15). RTA feeds into many different lytic and latent gene pathways, acting as both a positive and negative regulator of gene transcription. The many important functions exhibited by RTA make it one of the most tightly regulated genes in gammaherpesviruses where control is established through the use of alternative splicing, epigenetic modifications, feedback loops, and multiple promoters.

Recently we identified a new RTA promoter, which we named the distal gene 50 promoter (16). Notably, we previously showed that this promoter is also present in KSHV and EBV (Fig. 1). The transcript initiated from the distal promoter encodes a 181-bp exon (E0) at coordinates bp 65909 to 66089 in the MHV68 genome, which splices to the E1 exon located at coordinates bp 66509 to 66796 and then splices to exon 2 at coordinates bp 67662 to 69462. Notably, we have shown that a proximal gene 50 mutant virus is able to replicate, establish latency in both splenocytes and

peritoneal exudate cells (PECs), and reactivate from PECs, suggesting that the distal promoter is functional (16). However, the proximal-promoter mutant is defective in reactivation from splenocytes (16).

Here we demonstrate that the expression of RTA can be driven from multiple previously unknown promoters upstream of the distal promoter. These promoters encode three new exons, two of which represent extensions of exon 0 and the other a completely unique exon. To further characterize these promoters, we generated an MHV68 mutant lacking both the proximal and distal gene 50 promoters (G50DblKo). We show the G50DblKo virus retains the ability to replicate to levels similar to those for the wild-type (WT) virus, but only in the absence of a type I interferon (IFN) response. Furthermore, we show that the G50DblKo virus is extremely sensitive to type I interferons both *in vitro* and *in vivo*. We also show that despite the replication defect observed in the presence of a type I interferon response, the G50DblKo virus established a latent infection in both splenocytes and PECs, although it was unable to reactivate from either splenocytes or PECs. Importantly, the replication and latency defects exhibited by the G50DblKo mutant were largely rescued by infection of mice lacking a type I interferon response. Finally, despite the sensitivity of the G50DblKo mutant virus to type I IFNs, we show that the newly identified promoters themselves are not directly sensitive to IFN-α, indicating that type I IFNs likely act downstream of RTA transcription.

MATERIALS AND METHODS

Generation of G50DblKo and G50DblKo.MR viruses. The MHV68. G50DblKo virus was generated using the *galK*-mediated Red recombineering method as described previously (17, 18). Briefly, we introduced the MHV68 bacterial artificial chromosome (BAC) into the *galK* bacterial strain SW102, where the *galK* was inserted into the Orf50 locus. To generate the Orf50-*galK* swap, we amplified the *galK* gene from the plasmid pGalK using the primers GalK-G50-F (5′-CTTAAAGGAGGAG CTGTTGGCAGTGCTTGCTGAAAATACCTCATCAAACTCCTGTTG ACAATTAATCATCGGCA-3′) and GalK-G50-R (5′-CCTCAGCCTTT GAAGGGACATTTCATGACTCATGTAGGAGGAGCTACCAGTCAGC ACTGTC CTGCTCCTT-3′); this PCR product generated from pGalK includes 50 bp of homologous sequence upstream and downstream from the Orf50 locus. The PCR product was then introduced into the SW102 cells through electroporation, and those cells expressing recombinants were selected through the use of minimal medium with galactose. The ORF50/GalK recombinant BAC mutants (MHV68.Δ50galK) were confirmed through analyses using multiple restriction endonucleases.

To generate the G50DblKo virus, two separate PCRs with 25-μl reaction mixtures were performed on MHV68 WT BAC and 30 cycles using Phusion polymerase (New England BioLabs) and the following cycling conditions: 94°C for 30 s, 58°C for 30 s, and 72°C for 1 min. The primers used for reaction one amplification were forward primer Orf50F65040_65089 (5′-CTTAAAGGAGGAGCTGTTGGCA GTGCTTGCTGAAAATACCTCATCAAACT-3′) with reverse primer Orf50DpKo100RHindIII (5′-AATGGACTCCAGCTGAAGCTTAGT CATAGAACATACCATGA-3′), and the primers used for reaction two amplification were reverse primer Orf50R66641_66690 (5′-CCTCAG CCTTTGAAGGGACATTTCATGACTCATGTAGGAGGAGCTACCA G-3′) with forward primer Orf50DpKo100FHindIII (5′-GTATGTTC TATGACTAAGCTTCAGCTGGAGTCCATTATTCT-3′), generating overlapping PCR products to be used in round two amplification (of note, each internal primer contained a HindIII restriction enzyme site to be used for diagnostic purposes). Two microliters of each round one amplification product was then used as the template for a round two reaction using the external forward primer from reaction one

Orf50F65040_65089 and the reverse external primer from reaction two Orf50R66641_66690. The resulting product, containing a 50-bp deletion within the distal promoter region of the Orf50 locus, was gel purified and used as the template for a second overlapping PCR using the same conditions as the first PCR but this time targeting a deletion within the proximal promoter region. The primers used for reaction one amplification were forward primer Orf50F65040_65089 (5′-CTT AAAGGAGGAGCTGTTGGCAGTGCTTGCTGAAAATACCTCATC AAACT-3′) with reverse primer Orf50PpKORHindIII (5′-GAACAGT ATGAGAAAAAGCTTCAGGGAATTTTGTTATGTGC-3′), and the primers used for reaction two amplification were reverse primer Orf50R66641_66690 (5′-CCTCAGCCTTTGAAGGGACATTTCATG ACTCATGTAGGAGGAGCTACCAG-3′) with forward primer Orf50PpKoFHindIII (5′-CCCTGGAATCATAGAAAGCTTTTTCTCAT ACTGTTCCTTTT-3′). As before, 2 μl of each round one amplification product was used as the template for a round two reaction using the same external primers as before, Orf50F65040_65089 and Orf50R66641_66690. The resulting PCR product was gel purified and now contained a 50-bp deletion within the Orf50 distal promoter region, a 70-bp deletion within the Orf50 proximal promoter region, and 50 bp of homology to the region directly external to the MHV68.Δ50galK Orf50galK region. A WT Orf50 PCR product containing the 50-bp homology arms was also generated in order to create an Orf50 marker rescue of the MHV68.Δ50galK parent BAC to ensure that no spontaneous mutations had arisen. This mutant or WT PCR product was electroporated into SW102/MHV68.Δ50galK and after recombination was selected on minimal medium plates containing glycerol and 2-deoxy-D-galactose. The colonies were then screened by colony PCR using primers ORF50E0F (5′-CACAACCCAGCACATGTTCAAACAT-3′) and ORF50E0R (5′-CTGTGTCTCACTGAAAACACTC-3′). Colonies were then further verified by restriction digestion using the HindIII diagnostic sites, as well as confirmation by PCR of the ORF50 region and DNA sequencing of the PCR product (Macrogen Sequencing). The integrity of the nonmutated BAC was confirmed through further restriction endonuclease digestion using PstI and EcoRI. Restriction endonuclease digests were then subjected to Southern blotting analyses using a PCR-generated fragment spanning the entire Orf50 region as the probe.

Production of virus. Both the G50DblKo and G50DblKo.MR viruses were generated from yellow fluorescent protein (YFP) BAC (19). In order to ensure proper viral growth of the G50DblKo virus, a protocol was developed in which the virus would be passaged and titers determined in the absence of type I interferons. Both mutant and marker rescue BACs were transfected using LT-1 transfection reagent (Mirus) into Vero cells expressing Cre-recombinase (Vero-Cre cells). When cells reached 70% cytopathic effect (CPE), cells and supernatants were collected and freeze-thaw lysed three times. The resulting stock was used to infect new Vero-Cre cells to ensure the excision of the BAC. At 70% CPE, cells and supernatants were once again collected, lysed, and used to infect large quantities of Vero-Cre cells to scale up viral stocks. Viral titers were determined as described below.

Tissue culture. Mouse embryonic fibroblasts (MEFs) and NIH 3T12, Raw264.7, and Vero-Cre cells were maintained in Dulbecco's modified Eagle's medium (DMEM) supplemented with 10% fetal calf serum, 2 mM L-glutamine, 100 U of streptomycin per ml, and 100 U of penicillin per ml (cMEM). Vero-Cre cells used for virus generation were passaged with the addition of 300 μg of hygromycin B/ml. Cells were maintain at 37°C in a tissue culture incubator with 5% CO_2. MEFs were obtained from C57BL/6 mouse embryos, and IFN-α/βR$^{-/-}$ MEFs were obtained from 129S2/SvPas.IFN-α/βR$^{-/-}$ mice as previously described (20).

Growth curves, plaque assays, and viral titers. Growth curves were performed using Vero-Cre, 3T12, IFN-α/βR$^{-/-}$ MEF, or C57BL/6 MEF cells plated in six-well plates at a concentration of 1.75×10^5 cells per well 24 h prior to infection. The cellular concentration after 24 h was determined, and viral stocks were diluted to a 200 μl volume in cMEM at multiplicities of infection (MOIs) of 0.01, 0.1, and 10. These inoculums were added to the cellular monolayer, and plates were rocked every 15 min at 37°C for 1 h. After 1 h, fresh cMEM at a volume of 2 ml was added back to each well. The contents of the wells were collected at the indicated time points and frozen at −80°C until plaque assays were performed to determine titers. Growth curves with the addition of mouse recombinant IFN-α (Miltenyi Biotec) were performed in a similar manner, but IFN-α was added to the plated cells at a concentration of 10,000 IU/ml 1 h before infection. IFN-α was subsequently added at a concentration of 5,000 IU/ml every 24 h for the duration of the infection. Plaque assays were performed by plating Vero-Cre cells in six-well plates at a concentration of 1.75×10^5 cells per well 24 h prior to infection. Viral stocks or growth curve stocks at the indicated time points were freeze-thawed 3 times, and a 10-fold serial dilution was generated, 200 μl of each dilution was added to the Vero-Cre monolayer, and plates were rocked every 15 min at 37°C for 1 h. After 1 h, cells were overlaid with 2% fetal bovine serum (FBS) complete medium containing 20 g/liter methylcellulose (Sigma). Plaques were visualized at 14 days postinoculation by staining with neutral red (Sigma) at a concentration of 6% overnight.

RACE analysis. One-hundred-millimeter plates were seeded with Raw 264.7, Vero-Cre, or IFN-α/βR$^{-/-}$ MEF cells in cMEM and 24 h later were infected with WT-YFP or G50DblKo virus at an MOI of 5. Total RNA was isolated from these cells at 24 or 48 h postinfection using TRIzol reagent (Invitrogen). Five micrograms of RNA was DNase I treated (Invitrogen) and subjected to 5′ rapid amplification of cDNA ends (RACE) performed using the GeneRacer system (Invitrogen). RACE-ready cDNA was generated using Superscript III (Invitrogen) reverse transcription using random primers as per the manufacturer's instructions. RACE-ready cDNA was used to look for additional 5′ transcripts through the use of nested PCR utilizing Phusion high-fidelity *Taq* (NEB) and Platinum *Taq* (Invitrogen). Nested PCR was performed using the 5′ universal forward primer (round 1), the 5′ universal forward primer (round 2), and various reverse primers located in the Orf50 region: E2R1 (5′-ATTTCGAACAG ACTGCAGGCCAGAGGTTGA-3′), E2R2 (5′-CGAACATGGGGCAGT CAGAAACAGC-3′), E1R (5′-TTCAATTCTCATGGTCACATCT-3′), and E0R (5′-TTTGAACATGTGCTGGGTTGTG-3′). The following cycling conditions for Phusion *Taq* were used with 1 μl of cDNA in a 50-μl PCR mixture: 98°C for 30 s; 30 cycles of denaturing at 98°C for 10 s, annealing at 60°C for 30 s, and extension at 72°C for 1 min; and a final extension of 72°C for 10 min. Round 2 nested amplification was performed using 2 μl of round 1 product in a 50-μl reaction mixture using the same cycling conditions. The following cycling conditions for Platinum *Taq* were used with 1 μl of cDNA in a 50-μl PCR mixture: 95°C for 5 min; 30 cycles of denaturing at 94°C for 30 s, annealing at 60°C for 30 s, and annealing at 72°C for 1 min 30 s; and a final extension at 72°C for 7 min. Round 2 nested amplification was performed using 2 μl of round 1 product in a 50-μl reaction mixture using the same PCR conditions. PCR products were visualized through running on a 1% ethidium bromide gel, and excised bands were purified using a Geneclean II kit (MP Bio). Purified PCR products from Phusion PCR were ligated into a pCR-Blunt II TOPO vector (Invitrogen), and purified PCR products from Platinum *Taq* PCR were ligated into either a pCR4-TOPO vector (Invitrogen) or a pGEMT-Easy vector (Promega) and analyzed by DNA sequencing (Macrogen USA).

Cell transfections and luciferase assays. Transfection of Vero-Cre and RAW 264.7 cells was done in 6-well plates, where at 1 day prior to transfection, cells were plated at 2×10^5 cells per well in cMEM. Transfection mixtures were prepared using 2.5 μg of reported plasmid and 5 ng of pHR-LUC *Renilla* luciferase vector as a transfection control. Transfections were performed using LT-1 transfection reagent (Mirus) according to the manufacturer's instructions. pGL4.13[Luc] was used as a positive control, pGL4.10[luc] was used as a negative control, and the green fluorescent protein pMaxGFP was used to determine transfection efficiency. For assay mixtures treated with IFN-α, 5,000 IU/ml was added at 24 h posttransfection, and all cells were collected at 48 h posttransfection and lysed. All dual-luciferase assays were performed using a dual-luciferase kit

(Promega) according to manufacturer's instructions. Single-luciferase assays were performed using lab-made luciferase agent (1.5 mM HEPES [pH 8], 80 μM MgSO$_4$, 0.4 mM dithiothreitol [DTT], 2 μM EDTA, 10.6 μM ATP, 5.4 μM coenzyme A, and 9.4 μM beetle Luciferin), where 10 μl of cell lysate was added to 50 μl of luciferase agent. Both single- and dual-luciferase assays were read using a TD-20/20 luminometer (Turner Biosystems). All transfections were repeated in triplicate, and results are presented as a fold ratio over that for empty pGL4.10 vector.

Reporter plasmids and cloning. DNA from the Orf50 region was amplified from the MHV68 WT BAC and cloned into a luciferase reporter construct. Phusion *Taq* (NEB) was used with the following cycling parameters for all amplifications: 95°C for 5 min; 30 cycles of denaturing at 94°C for 30 s, annealing at 58°C for 30 s, and extension at 72°C for 30 s; and a final 72°C extension for 10 min. Overlapping PCR was used with the following primers to generate E0 luciferase promoter constructs with 50-bp deletions. Round one PCR used forward primer E0-250F (5′-GATCGGCTAGCTTAATCCTA TATGGAGAT-3′) with the following reverse primers: del 65822-65872R (5-CATGTCTCAGCCAACAGCTCGACACTTCGAGTACC-3′), del 65772-65822R (5′-AGAATAATGGACTCCAGCTGAGTCATAGAACATAC-3′), and del 65722-65772R (5′-GCACGTATTGCTGAAAAGGAATGATCAGG AATTCT-3′). Reverse primer E0ATGR (5′-GATCGAAGCTTGTGCTGGG TTGTGAAG-3′) was used with the following forward primers: del 65822-65872F (5′-GGTACTCGAAGTGTCGAGCTGTTGGCTGAGACATG-3′), del 65772-65822F (5′-GTATGTTCTATGACTCAGCTGGAGTCCATTAT TCT-3′), and del 65722-65772F (5′-AGAATTCCTGATCATTCCTTTTCA GCAATACGTGC-3′). After round one PCR, 2 μl of PCR products from del 65822-65872, del 65772-65822, and del 65722-65772 was used as the template for a round two PCR following the same cycling conditions as for round one with forward primer E0-250F and reverse primer E0ATGR. These second-round PCR products were gel purified and cloned into pCR-Blunt (Invitrogen) for vector shuttling and sequence confirmation. The pCR-Blunt plasmid was then cut with HindIII and NheI to excise the E0 fragments, and the luciferase reporter construct pGL4.10[luc2] (Promega) was also digested with HindIII and NheI. The digested E0 products and pGL4.10[luc2] vector were then gel purified, resuspended in Tris-EDTA (TE), and ligated together using T4 DNA ligase (NEB) overnight at 16°C. Ligation products were transformed into Top 10 chemically competent cells, and colonies were screened for the presence of correctly oriented E0 pGL4.10[luc2] vectors through restriction digestion and DNA sequencing. Clones containing correct E0 deletion and expression were cultured, and plasmid DNA was isolated using an Endofree Maxikit (Qiagen). The process of generating Orf50 N3 and N4/N5 promoter luciferase constructs followed a method similar to that described above, with only a single PCR amplification required to generate 1,000-bp-long PCR fragments. The primers used for this single PCR were as follows: the reverse primer N4_N5RBgl2 (5′-CGATAGATCTAAGCCGTGGTCAGCAGGT-3′) was used with the forward primer N4_N5F1000Nhe1 (5′-AGTCGCTAGCA ATCGTCCGGGGGGGTTAA-3′), and the reverse primer N3RBgl2 (5′-CGA TAGATCTAGCCTGGGGCATAGTTCTT-3′) was used with the forward primer N3FNhe1 (5′-AGTCGCTAGCTCAGGATGCAGTTAAGCA-3′). These products were gel purified, shuttled through pCR-blunt, digested with NheI and BglII, and then ligated into pGL4.10[luc2]. The generation of the proximal promoter expression constructs followed the same protocol as described above. Forward primer ProxPromF (5′-GATCGCTAGCTCTTTAT AGGTACCAGGGAA-3′) was used with reverse primer ProxPromR (5′-TA GCAGATCTGGTCACATCTGACAGAGAAA-3′) to generate the 410-bp proximal promoter luciferase construct. Overlapping PCR using forward primer ProxPromDelF (5′-CCCTGGAATCATAGATTTCTCATACTGTTC CTTTT-3′) with primer ProxPromR and reverse primer ProxPromDelR (5′-GAACAGTATGAGAAATCTATGATTCCAGGGAATTT-3′) with primer ProxPromF was used to generate the proximal promoter 70-bp deletion construct. Digestion, ligation, and purification also followed the same protocol as described above.

Limiting-dilution PCR and limiting-dilution reactivation assays. Limiting-dilution PCR to determine the frequency of viral genomes and a limiting-dilution CPE assay to determine the number of cells reactivating from latency were performed as previously described ([20], [21]). Briefly, to determine the frequency of viral genomes, splenocytes or PECs were serial diluted in 96-well plates and subjected to protease K digestion. After digestion, cells were used in a two-round nested PCR using primers found in the G50 region. PCR products were resolved on a 2% agarose gel and analyzed. To determine the frequency of infected cells reactivating from latency, splenocytes or PECs were counted and diluted in cMEM. Cells were then plated as serial 2-fold dilutions onto an MEF or IFN-α/βR$^{-/-}$ MEF monolayer in 96-well plates. In parallel, mechanically disrupted cells also were plated as a serial 2-fold dilution to detect any preformed infectious virus. At 21 days postplating, each well was assessed for CPE and scored as a percentage. For both limiting-dilution PCR and limiting-dilution reactivation, the Poisson distribution was used to determine frequencies.

Mice, infections, and tissue preparation. Female C57BL/6 mice (The Jackson Laboratory) and 129S2/SvPas.IFN-α/βR$^{-/-}$ mice 6 to 8 weeks of age were maintained at Emory University. Mice were housed under sterile conditions and maintained in accordance with Emory University School of Medicine (Atlanta, GA), as well as all federal guidelines. C57BL/6 or 129S2/SvPas.IFN-α/βR$^{-/-}$ mice were infected intranasally (i.n.) with 1,000 PFU of WT-YFP, G50DblKo, or G50DblKo.MR virus in 20 μl cMEM following isoflurane anesthetization. 129S2/SvPas.IFN-α/βR$^{-/-}$ mice were weighed at the time of infection, and weight was monitored daily; mice were sacrificed if they lost 20% of their original body weight. C57BL/6 mice were also infected intraperitoneally with 1,000 PFU of WT-YFP, G50DblKo, or G50DblKo.MR virus in 200 μl cMEM. With both routes of infection, C57BL/6 mice were sacrificed at day 18 postinfection or at 7 days postinfection for lung titers. Surviving 129S2/SvPas.IFN-α/βR$^{-/-}$ mice were sacrificed at day 28 postinfection. Mice were sacrificed by isoflurane and cervical dislocation. PECs were collected by peritoneal lavage using 10 ml cMEM, spleens were harvested, and splenocytes were prepared by manual homogenization, while lungs were harvested and prepared by mechanical bead disruption using 1.0-mm silica beads. Splenocytes were treated with Tris-ammonium chloride to eliminate red blood cells. All prepared cells were counted using a Cellometer Auto T4 (Nexcelom) and immediately used for lung titer, reactivation, or genome analysis. Cells not used immediately were stored in cMEM–10% dimethyl sulfoxide at −80°C.

Immunoblotting. Infections were carried out as described above for growth curves. At 24, 48, and 72 h postinfection, cells were harvested, washed with 1× phosphate-buffered saline (PBS), and then resuspended in 40 μl of lysis buffer containing 150 mM NaCl, 50 mM Tris-HCl, 1 mM EDTA, and 0.1% Triton X-100 supplemented with 1 mM NaF, 1 mM Na$_3$VO$_4$, and an EDTA-free protease inhibitor tablet (Roche). Protein quantifications were carried out using a DC protein assay (Bio-Rad). For all blots, 30 μg of protein was mixed with 6× SDS loading buffer, boiled for 5 min at 100°C, and resolved by SDS-PAGE. SDS-polyacrylamide gels were transferred to a nitrocellulose membrane using a semidry apparatus (Bio-Rad). After transfer, membranes were blocked in 5% milk in Tris-buffered saline (TBS)–Tween for 1 h at room temperature. After 1 h, membranes were washed three times with TBS-Tween, and the primary antibody rabbit anti-MHV68 RTA ([22]) diluted 1:1,000 in blocking buffer was added and left overnight with rocking at 4°C. Following overnight incubation, the primary antibody was removed and the membrane washed three times with TBS-Tween. The membrane was then incubated with the secondary donkey anti-rabbit antibody (Jackson Immunoresearch) diluted 1:2,000 in blocking buffer for 1 h at room temperature. This was followed by three additional washes with TBS-Tween. The blot was then developed using SuperSignal West Pico chemiluminescent substrate (Pierce). Membranes were stripped using Restore PLUS Western blot stripping buffer (Thermo Scientific). Membranes were then subjected to the same protocol using the primary mouse monoclonal β-actin antibody (Sigma) at 1:5,000 and the secondary donkey anti-mouse antibody (Jackson Immunoresearch) at 1:5,000. Membranes were also subjected to the same protocol to blot for v-cyclin, where primary rabbit
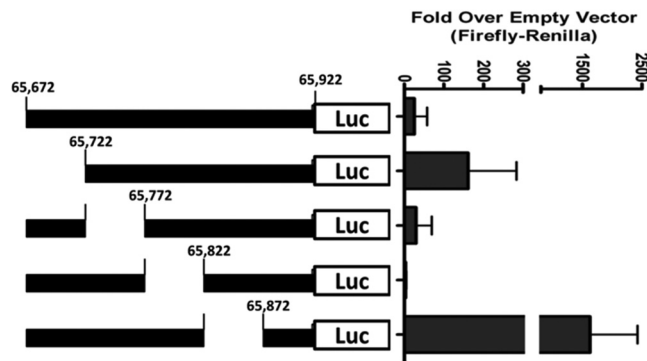
FIG 2 Promoter deletions within the MHV68 E0 250-bp promoter region. Reporter constructs were generated within the context of the 250-bp promoter through overlapping PCR. The 50-bp E0 promoter mutants were cloned into the pGL4.10[luc] luciferase report construct. RAW 264.7 cells were cotransfected with pGL4.10[luc] luciferase report constructs containing 50-bp deletions as illustrated and phRL-Luc (*Renilla* luciferase). RAW 264.7 cells were stimulated with LPS (5 μg/ml) at 24 h after transfection, and at 48 h after transfection luciferase assays were performed. Data are presented as the fold difference in the ratio of firefly to *Renilla* luciferase versus the pGL4.10[luc] empty vector control. The data were compiled from 3 independent transfections, each done in triplicate. Standard errors of the means are shown.

monoclonal v-cyclin antibody was used at 1:2,000 overnight and the secondary donkey anti-rabbit antibody (Jackson Immunoresearch) was used at 1:2,000 for 1 h at 4°C.

RESULTS

Characterization of the Orf50 distal promoter activity *in vitro*. We previously reported the generation and characterization of a gene 50 proximal promoter knockout virus (G50pKo), which led to the identification of an additional promoter upstream of the proximal promoter, now referred to as the distal promoter (16). The additional distal promoter drives the expression of a new exon (E0), and the core promoter region corresponds to the first 250 bp upstream of the E0 transcriptional start site. To further characterize the activity of this newly defined promoter region, we generated serial 50-bp deletions (Δ65672-65722, Δ65722-65772, Δ65772-65822, and Δ65822-65872) in the core 250-bp distal promoter region (Fig. 2). These serial 50-bp deletion fragments were cloned into the pGL4.10 luciferase reporter vector, and the resulting reporter plasmids transfected into RAW 264.7 cells. It was previously reported that the gene 50 distal promoter was most active in RAW 264.7 cells with the addition of lipopolysaccharide (LPS) (16).

Luciferase assays confirmed the previous finding that the 250-bp distal promoter region drives significant gene expression, ∼30-fold over that with empty vector in the RAW 264.7 cells with the addition of LPS (Fig. 2). Notably, deletion of the sequences from bp 65672 to 65722 resulted in a substantial increase in promoter activity over that with empty vector (∼4.6-fold above that observed with the full-length 250-bp promoter construct), indicating the presence of negative *cis* elements in this region. Similarly, deletion of the sequences from bp 65822 to 65872 also resulted in a strong enhancement of activity (∼40-fold above that observed with the full-length 250-bp promoter construct). This would indicate that both of these regions play an important role in limiting gene 50 transcription. Conversely, deletion of the sequences from bp 65772 to 65822 resulted in nearly complete si-

lencing of distal promoter activity (ca.16-fold below that observed with the full-length 250-bp promoter construct), arguing that essential positive *cis* elements map to this region. Therefore, we chose to delete the latter region in the context of the viral genome to ablate distal gene 50 promoter activity.

Generation of a recombinant MHV68 lacking both the proximal and distal gene 50 promoters. With the identification of a second promoter driving RTA expression, we set out to generate a gene 50 functionally null virus through the deletion of both the distal and proximal promoters. We targeted the promoter regions because previous attempts to propagate gene 50 null viruses harboring mutations within the coding sequence were confounded by the generation of wild-type revertant viruses upon growth on complementing cell lines (i.e., recombination of wild-type gene 50 sequences into the viral genome) (23). Since the gene 50 null mutants grow slowly on complementing cell lines, any wild-type revertant virus quickly overtakes growth of the gene 50 null virus and ends up dominating the viral stock generated. In a previous attempt to overcome this problem, we deleted a 183-bp region of the proximal gene 50 promoter (the only known gene 50 promoter at the time), and it was the analysis of this mutant virus that led to the identification of the distal gene 50 promoter (16). Notably, the deletion introduced into the viral genome to generate the proximal promoter mutant virus (G50pKo) also deleted the splice acceptor site utilized by the distal gene 50 promoter-driven gene 50 transcript. To circumvent this issue, we redesigned the proximal promoter deletion to introduce a 70-bp deletion (corresponding to the region immediately upstream of the exon 1 transcript at coordinates bp 66412 to 66482), leaving the splice acceptor site intact (Fig. 3A). This new gene 50 proximal promoter knockout virus (G50PpKo) was used as the backbone for the generation of the G50DblKo virus.

To disrupt the distal gene 50 promoter, we targeted the 50-bp region from bp 65772 to 65822, which was determined to be essential for promoter activity in the *in vitro* analyses carried out in the RAW 264.7 cell line (Fig. 2). To confirm the generation of the G50DblKo virus, we sequenced the areas of interest to ensure that the desired deletions were present in the viral genome (data not shown). To further confirm that the virus was intact and that the deletions were inserted into the gene 50 locus, as well as the absence of spontaneous rearrangements and insertions in the viral genome, we digested the mutant BAC with the restriction endonucleases HindIII, PstI, and EcoRI. Notably, in the process of generating the desired deletions, we introduced diagnostic HindIII sites (Fig. 3B and C). HindIII digestion of the G50DblKo mutant yielded the three expected digestion fragments (590 bp, 874 bp, and 1,059 bp), while HindIII digestion of wild-type virus and the marker rescue BAC DNAs resulted in the expected 2,643-bp product. To further assess the presence of the deletions in the gene 50 locus, we performed Southern blotting of the HindIII-digested BAC DNAs (Fig. 3C). We probed the blot with a 1,651-bp probe corresponding to genome coordinates from bp 65040 to 66690, which hybridized to all three fragments generated. Notably, the band intensities varied and were dependent on the extent that the probe overlapped with the fragments generated. Importantly, the wild-type-sized fragment was absent from the G50DblKo and G50PpKo viral genomes, eliminating the possibility of a genome duplication of the gene 50 locus or recombination of the targeting sequences into another region of the viral genome. The final confirmation that the mutant generated was specific to the area of interest was
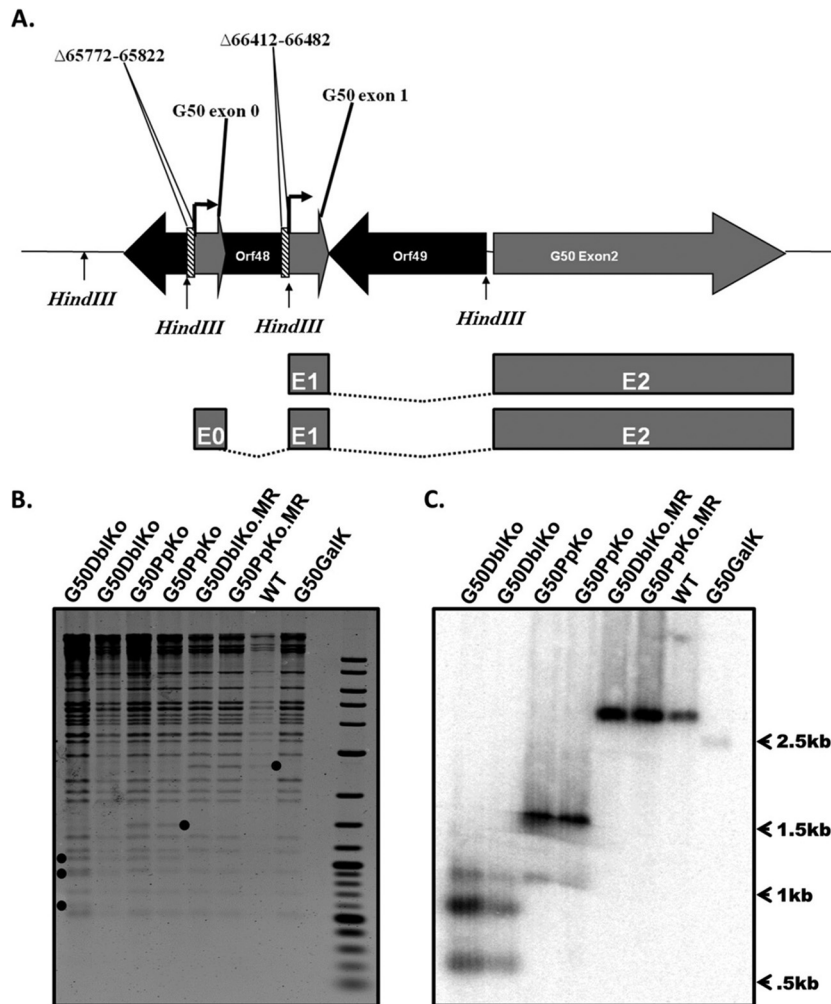
FIG 3 Generation of MHV68 G50DblKo and G50DblKo.MR viruses. (A) Schematic diagram of alternatively initiated gene 50 transcripts. The locations of the known proximal and distal gene 50 promoters are shown. The two hatched areas depict the regions deleted within the mutant G50DblKo virus: a 50-bp deletion extending from bp 65772 to 65822 in the distal promoter region and a 70-bp deletion extending from bp 66412 to 66482 in the proximal promoter region. There are two HindIII sites in the WT genome located at bp 64898 and 67541; the G50DblKo virus has two additional HindIII sites introduced within the deletions, located at bp 65797 and 66447. The splicing of E1 to E2 driven by the proximal promoter and the splicing of E0 to E1 to E2 driven by the distal promoter are shown. (B) HindIII restriction endonuclease digests of G50DblKo, G50PpKo, G50DblKo.MR, G50PpKo.MR, G50GalK, and WT-YFP BAC. The diagnostic restriction fragments are depicted (●). (C) Southern blot of the HindIII digest shown in panel B using a probe specific for the Orf50 region. Three unique digestion fragments are shown for the G50DblKo virus, the WT and MR rescue viruses are shown to be the same, and the *galK* parent fails to hybridize the Orf50 probe due to the Orf50 region replacement with the G50PpKo cassette.

the generation and confirmation of the G50DblKo.MR and G50PpKo.MR viruses, in which the Orf50 GalK region was replaced with the WT Orf50 region. These marker rescue viruses were all analyzed by sequencing, restriction enzyme digestion, and Southern blotting, and all three methods confirmed reversion back to WT virus. To ensure that the phenotypes observed with the G50pDblKo virus were in fact the result of the desired mutations, this process was conducted four independent times, resulting in the isolation of four independently generated mutant clones. These clones were used throughout the experiments interchangeably, and each experiment was conducted using at least two if not all of the clones. The use of multiple independent clones, in conjunction with the G50pDblKo.MR virus, makes it very unlikely that the observed phenotypes were the result of spontaneous mutations arising elsewhere within the genome.

Replication of the MHV68 G50DblKo mutant, but not wild-type MHV68, is inhibited by type I interferons. To generate the G50DblKo virus, the mutated BAC was first transfected into Vero cells expressing Cre recombinase (Vero-Cre cells) (24) to excise the BAC from the MHV68 BAC. The removal of the BAC sequence is necessary since virus containing BAC sequences is significantly attenuated *in vivo* (25). Upon successful removal of the BAC in Vero-Cre cells, viral stocks are generated by growth on murine NIH 3T12 cells (24). Surprisingly, Vero-Cre cells transfected with the G50DblKo BAC DNA supported growth of this mutant, indicating that the proximal and distal gene 50 promoters are not required for RTA expression. However, upon low-MOI infection of NIH 3T12 fibroblasts with the resulting viral stock generated from growth in Vero-Cre cells, we failed to observe any replication of the G50DblKo mutant. To further investigate this
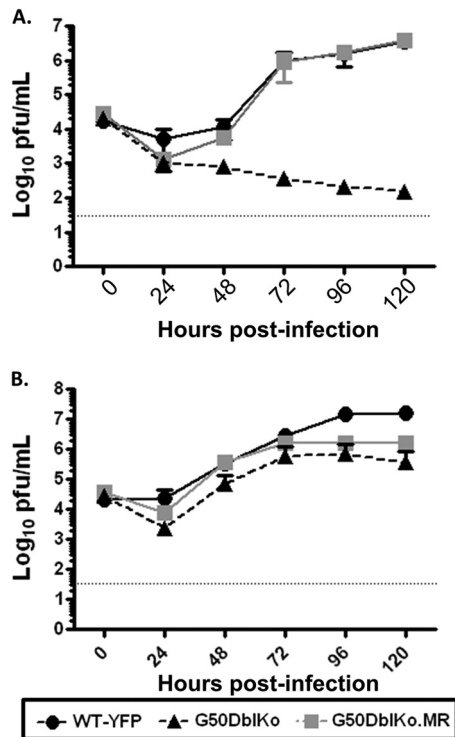
FIG 4 G50DblKo virus replicates *in vitro* in Vero-Cre cells but fails to replicate in NIH 3T12 fibroblasts. (A) Multistep growth curve of NIH 3T12 cells infected with an MOI of 0.1. Cells were infected with G50DblKo, G50DblKo.MR, and WT-YFP viruses and collected for viral titer analysis at the indicated times postinfection. (B) Multistep growth curve of Vero-Cre cells infected at an MOI of 0.1. Cells were also infected with G50DblKo, G50DblKo.MR, and WT-YFP viruses and collected for viral titer analysis at the indicated times postinfection.

phenomenon, multistep growth curves were performed on both NIH 3T12 and Vero-Cre cells (Fig. 4). Consistent with the initial analyses, the G50DblKo mutant was able to grow in Vero-Cre cells, exhibiting only a mild replication defect (Fig. 4B), indicating that both the proximal and distal gene 50 promoters are dispensable for RTA expression in these cells. However, we failed to observe any growth of the G50DblKo mutant on NIH 3T12 fibroblasts (ca. a 4- to 5-log defect in viral titers between the marker rescue virus and the G50DblKo mutant at late times postinfection) (Fig. 4A).

Since a major difference between Vero cells and NIH 3T12 fibroblasts is that Vero cells lack the ability to generate type I interferons, we assessed whether a type I IFN response can block replication of the G50DblKo mutant virus. We infected mouse embryo fibroblasts (MEFs) generated from C57BL/6 mice with the G50DblKo virus, and once again we failed to see efficient replication (Fig. 5A). The G50DblKo virus exhibited nearly a 4-log defect in viral titers at late times postinfection. To determine whether type I interferons were responsible for this large defect, we infected MEFs generated from 129S2/SvPas.IFN-α/βR$^{-/-}$ mice. Similar to the results obtained in Vero cells, the inability of the MEFs from mice lacking the IFN-α/β receptor to respond to a type I IFN response rescued the replication defect seen in the C57BL/6 MEFs (Fig. 5B). Notably, in the 129S2/SvPas.IFN-α/βR$^{-/-}$ MEFs, the G50DblKo virus replication was indistinguishable from that of wild-type virus (Fig. 5B). To directly examine the

impact of type I IFNs on replication of the G50DblKo mutant, we compared virus replication in Vero cells in the absence and presence of IFN-α. Vero-Cre cells were pretreated with IFN-α and then treated every 24 h postinfection. Cells that were not treated with IFN-α, as seen before, showed normal growth and kinetics of the G50DblKo virus, similar to those of WT and G50DblKo.MR viruses (Fig. 5C). However, adding IFN-α severely inhibited replication of the G50DblKo mutant (Fig. 5D).

These analyses revealed an impact of type I interferons on *in vitro* replication of MHV68 (although it has previously been shown that acute viral titers in the lungs of IFN-α/βR$^{-/-}$ mice are significant higher than those in wild-type mice and that the absence of a type I IFN response renders mice highly susceptible to lethal MHV68 infection [26–28]). These analyses also reveal that, despite replication of the G50DblKo virus being attenuated in the presence of a type I IFN response, there appears to be little or no replication defect in comparison to wild-type virus when a type I interferon response is absent, due to either the lack of the IFN-α/βR or the absence of type I IFN expression. In addition, these analyses demonstrate that despite the deletion of the known gene 50 promoters, the G50DblKo mutant is replication competent under some experimental conditions, suggesting that there are alternative mechanisms for expression of the essential immediate early RTA.

Notably, upon higher-MOI infections, although there was a partial rescue of the G50DblKo growth defect, this mutant still exhibited a pronounced growth defect (Fig. 6A). Consistent with the observed growth defect, we observed a small-plaque phenotype (Fig. 6C), which was observed with 4 independently derived G50DblKo mutant BAC clones, making it unlikely that any of the observed phenotypes are the result of secondary mutations in the viral genome. However, when we examined the levels of RTA protein as a function of time postinfection, we observed a faster kinetics and higher levels of RTA at early times postinfection (Fig. 6B, 8-hour time point). This correlated with higher levels of the v-cyclin expression as well at 8 hours postinfection (Fig. 6B). This argues that the defect in virus replication is not directly attributable to failure to express RTA protein, although it does suggest that entry into the lytic cycle may be dysregulated and that this could lead to a defect in virion production.

Identification of three additional gene 50 transcripts driven by 2 promoters mapping upstream of the distal gene 50 promoter. We have previously shown that transcription of MHV68 gene 50 is driven by two distinct promoters: (i) the proximal promoter, encoding a short 288-bp exon, E1, which splices to the large 1,800-bp exon, E2 and (ii) the distal promoter, which encodes a short 181-bp exon, E0, which splices to E1, which in turn splices to E2 (6, 12, 16) (Fig. 1). We further showed that this organization of gene 50 transcription was conserved in both EBV and KSHV (16). The unexpected ability of the G50DblKo mutant to replicate under some experimental conditions indicated that there must exist alternative mechanisms for driving gene 50 transcription, since RTA is known to be absolutely required for virus replication (this has been shown for EBV, KSHV, and MHV68) (23, 29–32). To determine if this hypothesis was indeed correct, we performed 5′ RACE analysis of RNAs from Vero-Cre, RAW 264.7, and IFN-α/βR$^{-/-}$ MEFs infected with either wild-type MHV68 or the G50DblKo mutant. From this analysis, we were able to detect three previously unidentified gene 50 transcripts
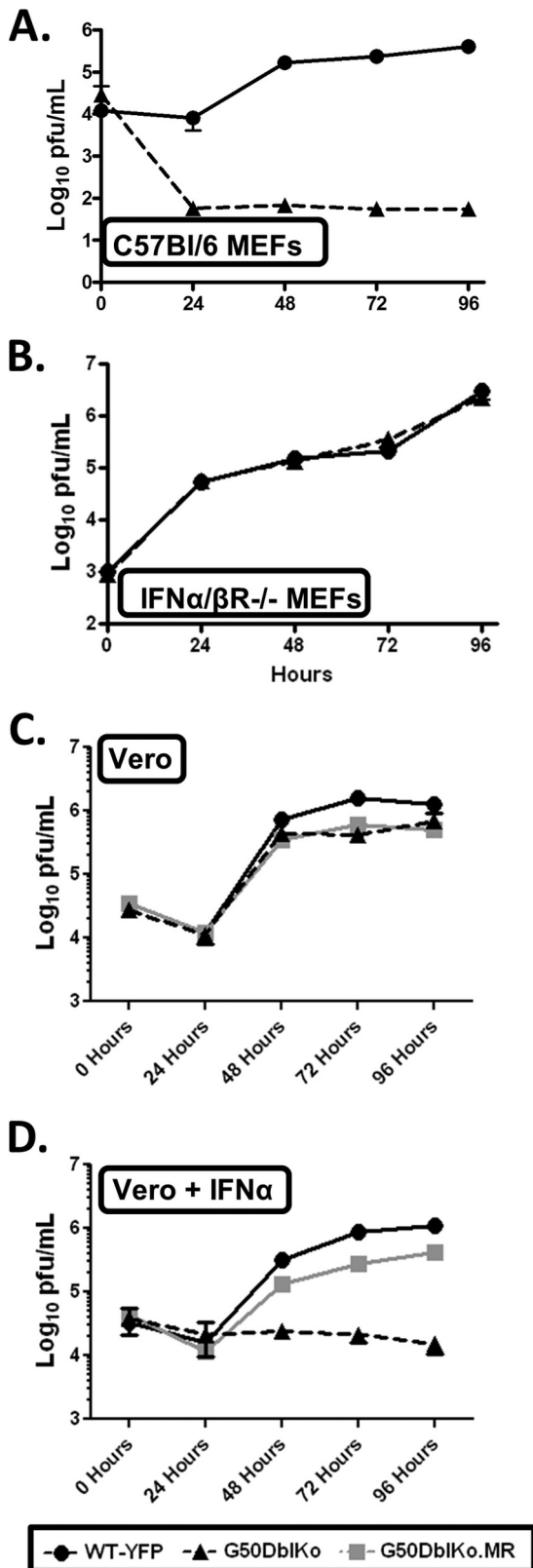
FIG 5 G50DblKo virus fails to replicate *in vitro* when IFN-α is present. (A) Multistep growth curve of C57BL/6 mouse embryonic fibroblasts (MEFs) infected with G50DblKo or WT-YFP virus at an MOI of 0.01. (B) Multistep growth curve of 129S2/SvPas.IFN-α/βR⁻/⁻ mouse embryonic fibroblasts (IFN-α/βR⁻/⁻ MEFs) infected with G50DblKo or WT-YFP virus at an MOI of
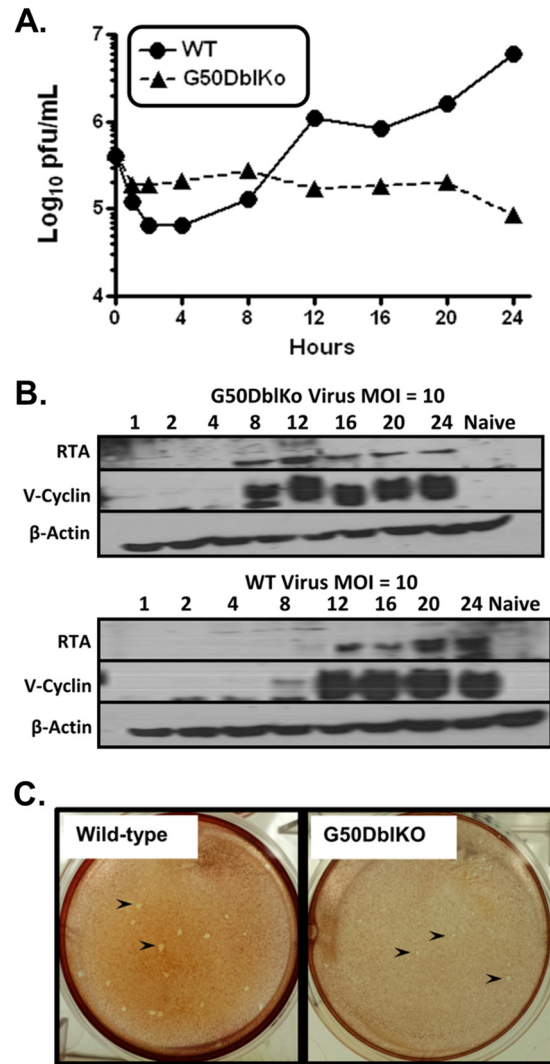

FIG 6 Single-step growth analyses of the G50pDblKo mutant and analysis of the kinetics of RTA expression. (A) Single-step growth curve of G50pDblKo or WT-YFP virus in NIH 3T12 fibroblasts infected at an MOI of 10. (B) Western blot staining for RTA, v-cyclin, and β-actin expression from the same cells used in the single-step growth curve shown in panel A. (C) Representative sample of the small-plaque phenotype exhibited under all experimental conditions when using different G50pDblKo clones.

which initiated from two distinct upstream transcription initiation sites (Fig. 7).

The three additional transcripts were identified in all three cell types examined and also were identified in both wild-type MHV68- and G50DblKo virus-infected cells. It is important to note that the 5′ RACE analyses conducted using the G50DblKo virus failed to detect the presence of any E1-E2 or E0-E1-E2 transcripts, further confirming that G50DblKo is indeed a true knock-

0.01. (C) Multistep growth curve of Vero-Cre cells infected with G50DblKo, G50DblKo.MR, or WT-YFP virus at an MOI of 0.1. (D) Multistep growth curve of Vero-Cre cells, treated with IFN-α (10,000IU/ml) at the time of infection and every 24 h thereafter, infected with G50DblKo, G50DblKo.MR, or WT-YFP virus at an MOI of 0.1. All cells were collected at the times indicated, and experiments were repeated at least in triplicate.
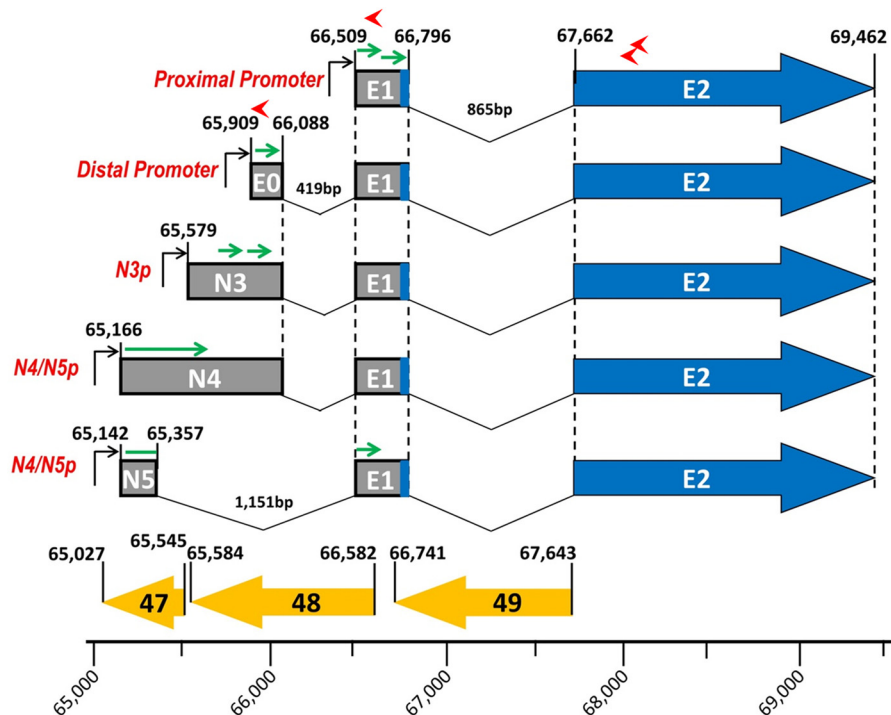
FIG 7 RACE analyses reveal three additional G50 exons upstream of E0. RACE analyses were performed using cDNAs generated from WT-YFP- and G50DblKo-infected Vero-Cre, Raw 264.7, and IFN-α/βR$^{-/-}$ MEFs at 24 and 48 h postinfection. 5′ RACE analysis using reverse primers located in E2, E1, and E0 were used in conjunction with the universal 5′ RACE forward primer. All three experiments identified three additional exons upstream of E0: exon N3, representing a 330-bp extension of E0; exon N4, representing a 743-bp extension of E0; and exon N5, representing a small novel 216-bp exon. All three new exons follow canonical splicing in which they splice to E1, which in turn splices to E2. Green arrows denote short ATG-initiated open reading frames that lie upstream of the RTA-coding sequences, which are indicated in blue. The locations of the major open reading frames antisense to gene 50 are also shown. Red arrows denote primers used in the 5′ RACE analyses. The positions of the primers used were as follows: E2-1, bp 68095 to 68066; E2-2, bp 68051 to 68027; E1, bp 66530 to 66509; and E0, bp 65930 to 65909.

out of the proximal and distal gene 50 promoters. The first new exon, which we have termed N3, is a 330-bp extension of the previously characterized E0 exon. This new N3 exon is 511 bp long and maps to coordinates bp 65579 to 66090 in the MHV68 genome. The 3′ end of this exon is identical to the 3′ end of the E0 exon. Like E0, this newly identified N3 exon splices to the E1 exon, leading to removal of a 419-bp intron, which in turn splices to the E2 exon, removing an 865-bp intron (Fig. 7). The second new exon, which we have termed N4, is a 743-bp extension of the E0 exon. The N4 exon map to bp 65166 to 66090 in the MHV68 genome and is 924 bp long (Fig. 7). The 3′ end of this exon is also identical to the 3′ end of E0 and splices to the E1 exon and then to the E2 exon. The final alternatively spliced transcript contains a new exon, which we have termed N5, which is 216 bp long and maps to bp 65142 to 65358 in the MHV68 genome (Fig. 7). This new exon consists mainly of the 5′ end of the newly identified N4 exon, with a 24-bp extension, indicating that the N4 and N5 exons share a promoter region. However, unlike N4, which is an extension of E0, the N5 exon exhibits a completely unique splicing event in which the 3′ end at bp 65358 splices to E1, directly eliminating a large 1,151-bp intron. Like the other known exons, the E1 exon then splices to the E2 exon.

It is important to note that none of the newly identified exons have been observed to splice directly to the E2 exon, but rather all of them splice to the E1 exon, which contains the RTA translation initiation codon. Thus, to date, there is no evidence for alternative

RTA translation initiation sites. This, however, does not exclude the possibility of unique splicing events from the newly identified transcripts to a novel position within the E2 exon or elsewhere within the viral genome. It should be noted that there are several short ATG-initiated open reading frames within the newly identified exons, which may play an important role (i.e., encoding novel viral gene products and/or interfering with RTA translation) (Fig. 7).

Neither the N3 promoter nor the N4/N5 promoter exhibits sensitivity to IFN-α, but RTA levels from the G50DblKo mutant are diminished in the presence of a type I IFN response at low MOI. The identification of alternative gene 50 transcripts provides a clear mechanism by which the G50DblKo virus is apparently able to generate sufficient levels of RTA to drive virus replication, at least in the absence of a type I IFN response. However, it does not address the issue of why replication of the G50DblKo mutant is suppressed by type I IFNs. To begin to address this issue, we cloned 1,000-bp fragments immediately upstream of the 5′ ends of the N3 and N4/N5 transcripts into the pGL4.10 luciferase reporter vector (Promega Biotech) and transfected the resulting reporter constructs into Vero-Cre cells. While the N3 promoter resulted in expression ~4-fold over that with empty vector, the N4/N5 promoter resulted in slightly higher levels of luciferase expression (~13-fold over empty vector) (Fig. 8). These data demonstrate that the region immediately upstream of the newly identified gene 50 transcripts exhibits modest promoter activity.
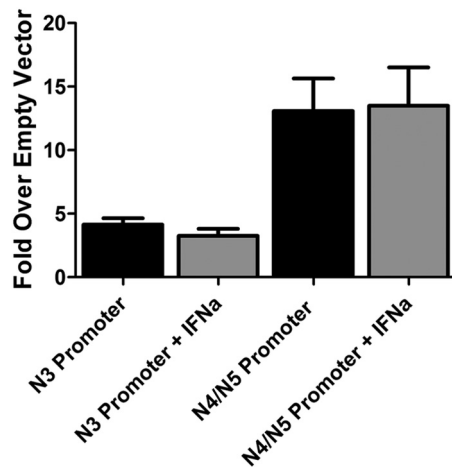
FIG 8 Promoter activity in the region immediately 5′ to MHV68 N3, N4, and N5 exons. Vero cells were transfected with pGL4.10[luc] luciferase report constructs containing either 1,000 bp upstream of N3 or 1,000 bp upstream of the N4/N5 exon. Vero cells were stimulated with IFN-α (10,000 IU/ml) at 24 h after transfection, and at 48 h after transfection luciferase assays were performed. Data are presented as the fold difference of firefly luciferase activity versus the pGL4.10[luc] empty vector control. The data represent triplicates of at least three independent transfections.

To determine if the type I IFN-sensitive replication of the G50DblKo mutant virus reflects type I IFN-mediated suppression of gene 50 transcription from the G50DblKo mutant, we examined N3 and N4/N5 promoter activity in the presence of IFN-α treatment (Fig. 8). Since Vero cells fail to produce IFN-α but retain the ability to respond to exogenously added IFN-α (Fig. 5D), IFN-α was added to the transfected Vero cells and promoter activity assessed (Fig. 8). Similar luciferase assays of previously identified Orf50 transfected promoters have shown them to be sensitive to IFN-γ (33). However, our analysis showed no evidence of IFN-α suppression of reporter gene activity, suggesting that IFN-α inhibition of G50DblKo replication acts downstream of gene 50 transcription. This is consistent with the absence of any consensus IFN-stimulated response elements (ISREs) in the region upstream of the N3 and N4/N5 transcription initiation sites.

Since it appeared that the newly identified gene 50 promoters are not sensitive to IFN-α, we examined the levels of RTA protein expression in wild-type MHV68- and G50DblKo mutant-infected cells. To assess RTA levels following infection, immunoblots were probed at several time points following low-MOI infection (Fig. 9). Consistent with the observed replication defect of the G50DblKo mutant virus in either NIH 3T12 fibroblasts or C57BL/6 MEFs, RTA levels were lower at all time points assessed (Fig. 9A and B). However, equivalent levels of RTA were detected in 129S2/SvPas.IFN-α/βR⁻/⁻ MEFs infected with either wild-type MHV68 or the G50DblKo mutant virus. It is also notable that RTA was readily detectable by 24 h postinfection of either C57BL/6 MEFs or 129S2/SvPas.IFN-α/βR⁻/⁻ MEFs but not NIH 3T12 fibroblasts (compare Fig. 9B and C with A). We have previously noted that MEFs are more sensitive to MHV68 infection as determined by a limiting-dilution CPE analysis which can detect between 0.1 and 0.2 PFU of virus with titers determined on NIH 3T12 fibroblasts (34), and this likely accounts for the earlier detection of RTA expression (i.e., effectively a higher-MOI infection).
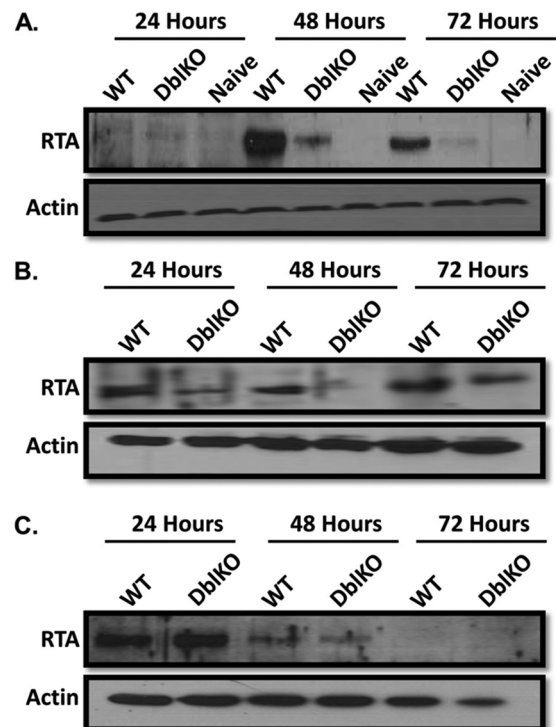

FIG 9 Immunoblot analyses of RTA protein expression levels in WT- and G50DblKo-infected NIH 3T12 fibroblasts, C57BL/6 MEFs, and 129S2/SvPas.IFN-α/βR⁻/⁻ MEFs. (A) NIH 3T12 cells were infected with wild-type MHV68 or the G50DblKo mutant at an MOI of 0.1, and cells were harvested at 24, 48, and 72 h postinfection. Cells were lysed, and 30 μg of protein was used for the immunoblot analyses to assess RTA expression levels. (B and C) MEFs prepared from either C57BL/6 (B) or 129S2/SvPas.IFN-α/βR⁻/⁻ (C) were infected at an MOI of 0.1, and cells were harvested at 24, 48, and 72 h postinfection. As for panel A, cells were then lysed and 30 μg of protein used in a immunoblot analysis to detect RTA expression levels. All immunoblots were stripped and then reprobed for β-actin levels to ensure equal protein loading.

When looking at RTA levels from growth curves following high-MOI infection, in which there is a partial rescue of the G50DblKo growth defect (Fig. 6A), the early kinetics and expression of RTA appear to be at similar or slightly higher levels than in WT infection (Fig. 6B). RTA was detectable at significant levels at 8 h postinfection in the G50DblKo virus-infected fibroblasts, while RTA was detectable at 12 h postinfection in WT virus-infected fibroblasts. However, the levels of RTA begin to wane by 24 h postinfection with the G50DblKo mutant, while WT RTA continues to increase. This may help explain the partial rescue of the growth phenotype at high MOI. Notably, the induction of v-cyclin expression parallels that of RTA expression for both the WT and G50DblKo infections. These results demonstrate that despite an increased sensitivity to type I interferons, as well as a partial growth defect at high MOI, the G50DblKo virus is able to generate functional RTA capable of driving transcription as well as launching expression of downstream viral targets such as v-cyclin.

The G50DblKo mutant establishes latency in the spleen and in PECs but is severely impaired for virus reactivation. To assess infection in mice with the G50DblKo mutant, we initially infected C57BL/6 mice intranasally with 1,000 PFU of either the G50DblKo virus, WT MHV68, or the G50DblKo.MR virus. We then assessed viral latency at day 18 postinfection, the peak of
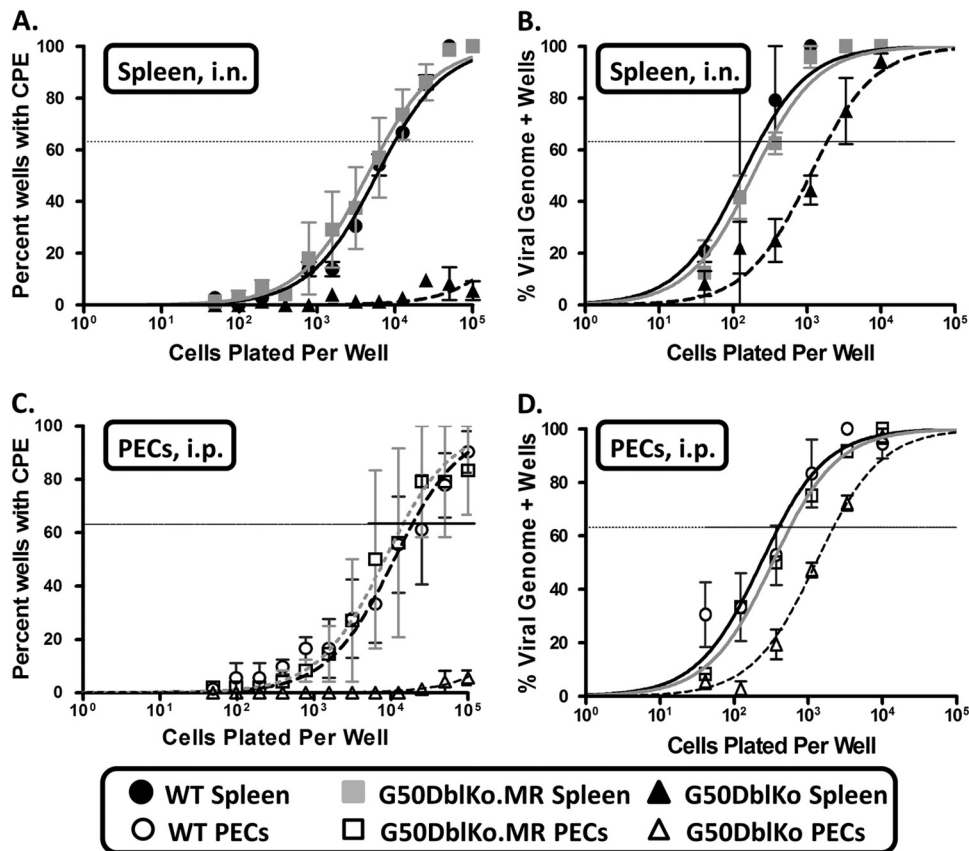
FIG 10 G50DblKo virus exhibits a severe reactivation defect and a moderate latency defect *in vivo*. Female C57BL/6 mice were infected with 1,000 PFU i.n. (A and B) or with 1,000 PFU i.p. (C and D). Splenocytes and PECs were harvested at 18 days postinfection and assessed for the establishment of latency and reactivation from latency by limiting-dilution CPE and PCR assays. (A) Splenocytes from i.n. infections were plated in serial dilutions onto an IFN-α/βR$^{-/-}$ MEF monolayer, and at 21 days postplating wells were individually scored for CPE. The percentage of these wells was used to calculate the frequency of virally reactivating cells. (B) Splenocytes from i.n. infections were plated in serial dilutions and subjected to nested PCR to detect gene 50 copies. The percentage of genome-positive cells in each dilution was used to calculate the frequency of latency. (C) PECs from i.p. infections were plated in serial dilutions onto an IFN-α/βR$^{-/-}$ MEF monolayer, and 21 days postplating wells were individually scored for CPE. The percentage of these wells was used to calculate the frequency of virally reactivating cells. (D) PECs from i.p. infections were plated in serial dilutions and subjected to nested PCR to detect gene 50 copies. The percentage of genome-positive cells in each dilution was used to calculate the frequency of latency. For all reactivation assays (A and C), mechanically disrupted cells were plated in parallel for each virus shown to control for preformed infectious virus, and all mechanically disrupted cells were negative for reactivation (data not shown). Data are representative of at least two independent experiments consisting of 5 mice per group. Error bars indicate the standard error of the mean.

latency in the spleen, and determined both the frequency of splenocytes harboring the viral genome and the frequency of splenocytes able to reactivate from latency. Splenocyte reactivation was determined by the previously described limiting-dilution CPE assay (20) modified by plating splenocytes on IFN-α/βR$^{-/-}$ MEF monolayers to ensure the ability to detect any reactivated G50DblKo mutant virus. The reactivation analyses revealed the nearly complete absence of detectable reactivation of the G50DblKo virus from splenocytes (Fig. 10A). In contrast, splenocytes harvested from wild-type virus-infected animals reactivated at a frequency of 1 in 7,035 cells, while the frequency of reactivation from the G50DblKo.MR virus was 1 in 9,549 cells (Fig. 10A and Table 1). No preformed infectious virus was detected in the harvested splenocyte samples, as measured by mechanical disruption of the cells as previously described (20) (data not shown).

To determine if this failure to reactivate from splenocytes observed with the G50DblKo mutant virus was the result of a failure to establish latency, limiting-dilution PCR was performed to determine the frequency of splenocytes harboring viral genomes

(20). We observed that the frequency of splenocytes harboring latent virus was roughly equivalent for the wild-type virus and the G50DblKo.MR virus at 1 in 223 and 1 in 305 cells, respectively, while the G50DblKo mutant virus was present in splenocytes at a frequency of ca. 1 in 1,941 cells (Fig. 10B and Table 1). While the frequency of viral genome-positive splenocytes in the G50DblKo virus-infected animals was around 8.5-fold lower than that in the wild-type virus-infected animals, these analyses demonstrate that this mutant virus is able to get to the spleen and establish latency. Thus, the lack of detectable reactivation of the G50DblKo mutant reflects a significant defect in virus reactivation from B cells, the dominant latently infected cell population in the spleen (19, 35).

We extended these analyses to address whether the inability of the G50DblKo mutant virus to reactivate from splenocytes was dependent on the route of inoculation and to assess latency and reactivation from PECs. To do this we assessed virus reactivation from splenocytes and PECs following intraperitoneal (i.p.) inoculation. C57BL/6 mice were infected by intraperitoneal inoculation with 1,000 PFU of G50DblKo, wild-type, or G50DblKo.MR

TABLE 1 Summary of virus latency and reactivation

Mouse	Route	Day	Virus	Splenocytes		PECs	
				Reactivation	Latency	Reactivation	Latency
C57BL/6	i.n.	18	WT	1 in 7,035	1 in 223	ND[a]	ND
			MR	1 in 9,549	1 in 305	ND	ND
			DblKo	Undetectable	1 in 1,941	ND	ND
	i.p.		WT	1 in 36,107	1 in 388	1 in 17,782	1 in 401
			MR	1 in 65,962	1 in 1,047	1 in 14,417	1 in 562
			DblKo	1 in 422,863	1 in 627	Undetectable	1 in 2,137
IFNαβR$^{-/-}$	i.n.	28	WT[b]	1 in 77,624	1 in 131	ND	ND
			DblKo	1 in 52,420	1 in 133	ND	ND

[a] ND, not determined.
[b] Latency and reactivation were determined by pooling splenocytes from the 3 IFNαβR$^{-/-}$ mice that survived wild-type MHV68 infection.

virus, and splenocytes and PECs were harvested at 18 days postinfection. We first examined the ability of the virus to reactivate from splenocytes, as described above. As observed following intranasal inoculation, the G50DblKo mutant exhibited a large defect in reactivation, although a low but significant level of virus reactivation was detectable (it was estimated by extrapolation that the G50DblKo mutant reactivates at a frequency of 1 in 422,863 splenocytes) (Table 1). In these analyses, wild-type virus reactivated at a frequency of 1 in 36,107 splenocytes, while the G50DblKo.MR virus reactivated at a frequency of 1 in 65,962 splenocytes (Table 1). Notably, the frequency of splenocytes reactivating virus at day 18 following intraperitoneal inoculation was 5- to 7-fold lower than that observed at the same time point following intranasal inoculation. This likely reflects faster kinetics of establishment and contraction of splenic latency following intraperitoneal inoculation. This effect, coupled with the observed low-level reactivation of the G50DblKo mutant, provides evidence that the route of inoculation does have an impact on reactivation of this mutant virus, which could be linked to better establishment of B cell latency (see discussion below). We then assessed whether the observed reactivation defects correlated with a defect in the establishment of latency. Notably, the 8.5-fold defect in establishment of latency in splenocytes observed following intranasal inoculation was largely rescued following intraperitoneal inoculation (Table 1). The frequency of viral genome-positive cells in the splenocytes following intraperitoneal inoculation was 1 in 388 cells for wild-type MHV68, 1 in 1,047 cells for the G50DblKo.MR virus, and 1 in 627 cells for the G50DblKo mutant (Table 1).

While nearly all virus reactivation from splenocytes arises from latently infected B cells (21, 36), macrophages represent the major latently infected cell type in PECs. Thus, to address whether the observed defect in G50DblKo reactivation from splenocytes reflects a B cell-specific defect, we determined the frequency of PECs reactivating virus. In contrast to the previous observation that the G50pKo virus retained the ability to reactivate from PECs (16), G50DblKo exhibited no detectable reactivation from PECs (Fig. 10C and Table 1). As expected, both wild-type MHV68 and the G50DblKo.MR virus reactivated from PECs, at frequencies of 1 in 17,782 cells and 1 in 14,417 cells, respectively (Fig. 10C and Table 1). These results indicate that despite the ability to drive viral replication, the absence of both the proximal and distal gene 50 promoters results in a substantial impairment in the ability of MHV68 to reactivate from infected

cells *in vivo*. Despite rescue of establishment of latency in splenocytes following intraperitoneal inoculation, a ca. 6-fold defect in the establishment of latency in PECs was observed (the frequency of viral genome-positive PECs in wild-type-infected animals was 1 in 401 cells, in G50DblKo.MR-infected animals it was 1 in 562 cells, and in G50DblKo-infected animals it was ca. 1 in 2,137 cells) (Fig. 10D and Table 1). Despite the modest impairment of the G50DblKo mutant in the establishment of latency in PECs, it is clear that this mutant is significantly impaired in reactivation from latency from both splenic B cells and peritoneal macrophages.

The G50DblKo phenotype *in vivo* is partially rescued in mice lacking the IFN-α/β receptor. Since we have shown that the G50DblKo mutant virus retains the ability to grow with normal kinetics and to high titer in cells that lack a type I IFN response (Fig. 4B and 5B), we assessed whether the absence of a type I IFN response *in vivo* would rescue the G50DblKo replication and reactivation defects. Thus, we infected 129S2/SvPas.IFN-α/βR$^{-/-}$ mice with 1,000 PFU of either the G50DblKo mutant or wild-type MHV68 via intranasal inoculation. It has previously been shown that MHV68 infection of mice lacking the IFN-α/β receptor results in the majority of mice succumbing during the acute phase of infection (26–28, 37). Surprisingly, while the G50DblKo mutant replicated to high titers in the lungs of IFN-α/βR$^{-/-}$ mice (Fig. 11C), all infected mice survived (Fig. 11A). However, as expected, only 3 of 19 mice infected with 1,000 PFU wild-type MHV68 WT virus survived past 2 weeks postinfection (Fig. 11A). Parallel analyses in C57BL/6 mice confirmed the severe replication defect observed with the G50DblKo mutant (virus replication in the lungs was below the limit of detection in all infected mice). Notably, acute replication of the G50DblKo mutant in the lungs of IFN-α/βR$^{-/-}$ mice was rescued to near-wild-type MHV68 levels (Fig. 11C). To further address the absence of lethality in IFN-α/βR$^{-/-}$ mice with the G50DblKo mutant, we extended these studies using higher inoculating doses. We did not observe any lethality, even when mice were infected with a ca. 400-fold-higher dose of the G50DblKo mutant (5 of 5 mice infected survived for greater than 4 weeks postinfection) (Fig. 11D). Thus, while acute virus replication of the G50DblKo mutant in the lungs following intranasal inoculation was largely rescued by loss of a type I IFN response, MHV68-associated lethality was not observed, indicating a requirement for the gene 50 proximal and/or distal promoter for RTA expression in some anatomical site during the acute phase of virus infection.
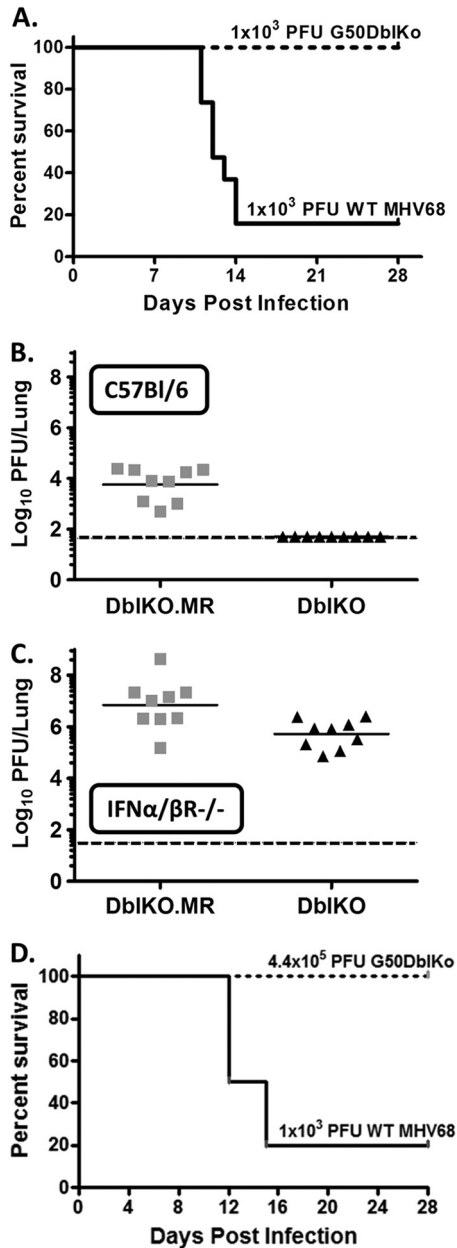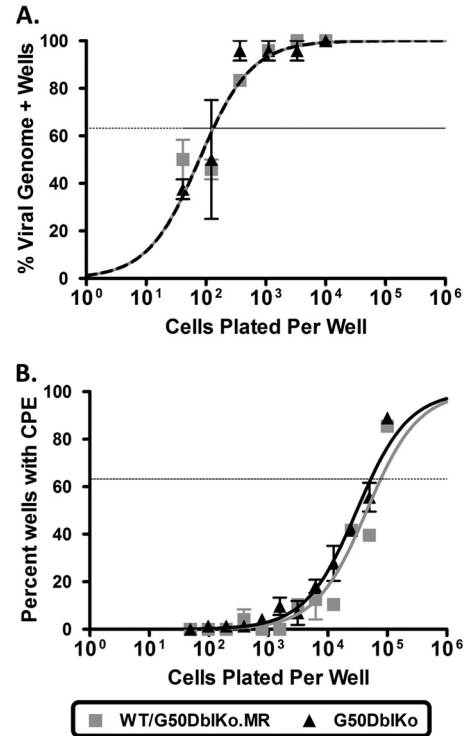
FIG 12 G50DblKo virus establishes latency and reactivates to similar levels as WT virus when used to infect 129S2/SvPas.IFN-α/βR$^{-/-}$ mice *in vivo*. Female 129S2/SvPas.IFN-α/βR$^{-/-}$ mice were infected with 1,000 PFU of G50DblKo virus, WT virus, or G50DblKo.MR virus by intranasal injection. Mice surviving at day 28 postinfection (n = 20 for G50DblKo; n = 3 for WT/G50DblKo.MR) were harvested for splenocytes and assessed for establishment of latency and reactivation from latency. (A) As for Fig. 10A, splenocytes were serially diluted and used in a CPE assay to look for the frequency of viral reactivating cells. (B) As for Fig. 10B, splenocytes were serially diluted and used in a nested PCR assay to look for the frequency of viral genome-positive cells.

FIG 11 Infection of 129S2/SvPas.IFN-α/βR$^{-/-}$ mice with G50DblKo virus does not result in lethality as seen with WT virus, despite the presence of high viral titers in the lungs. (A) Kaplan-Meier curve depicting survival of 129S2/SvPas.IFN-α/βR$^{-/-}$ mice when challenged with 1,000 PFU i.n. of WT or G50DblKo virus. (B) Lung titers at day 7 from C57BL/6 mice infected with 1,000 PFU i.n. of G50DblKo or G50DblKo.MR virus. (C) Lung titers at day 7 from 129S2/SvPas.IFN-α/βR$^{-/-}$ mice infected with 1,000 PFU i.n. of G50DblKo or G50DblKo.MR virus. (D) Kaplan-Meier curve depicting survival of 129S2/SvPas.IFN-α/βR$^{-/-}$ mice when challenged with 440,000 PFU i.n. of G50DblKo virus compared to survival of mice when challenged with 1,000 PFU G50DblKo.MR virus.

Having shown that the severe defect in acute replication of the G50DblKo mutant observed in C57BL/6 mice was largely rescued in mice lacking the ability to respond to type I IFNs, we assessed establishment of latency and virus reactivation in IFN-α/βR$^{-/-}$ mice. Spleens were harvested at day 28 from IFN-α/βR$^{-/-}$ mice intranasally infected with 1,000 PFU of either wild-type or

G50DblKo virus. It is important to note that the latency and reactivation analyses for wild-type virus-infected IFN-α/βR$^{-/-}$ mice were carried out using the subset of infected animals that survived acute virus replication (Fig. 10A). Like the rescue of acute virus replication in the lungs, the frequency of viral genome-positive splenocytes went from a ca. 8-fold defect in i.n. infected C57BL/6 mice (Fig. 10B) to an almost identical frequency of virus-infected splenocytes in IFN-α/βR$^{-/-}$ mice (1 in 131 cells for wild-type MHV68 and 1 in 133 for the G50DblKo mutant) (Fig. 12A and Table 1). More importantly, the defect in virus reactivation observed in C57BL/6 mice was completely rescued in IFN-α/βR$^{-/-}$ mice (1 in 77,624 splenocytes in WT-infected mice compared to 1 in 52,420 splenocytes in G50DblKo virus-infected mice) (Fig. 12B and Table 1). The latter result argues in favor of a model in which the sole defect in G50DblKo virus reactivation from C57BL/6 splenocytes is the inability to overcome type I IFN suppression of virus replication.

One possible explanation for the ability of the G50DblKo virus to replicate in the absence of type I interferons would be an increased expression of E1-E2 transcripts. This would make the G50DblKo virus not a true double promoter knockout virus, as E1-E2 transcripts would be responsible for the ability of the virus to replicate. However, this does not appear to be the case because (i) as shown in Fig. 6, RTA expression from the G50DblKo in
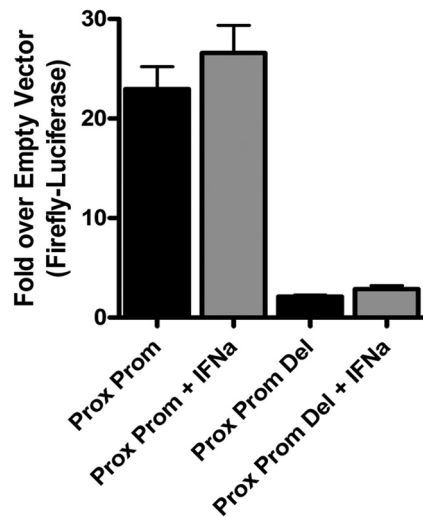
FIG 13 Promoter activity in the region immediately 5′ to the MHV68 proximal promoter and proximal promoter deletion. Vero cells were transfected with pGL4.10[luc] luciferase reporter constructs containing either 410 bp upstream of exon 1 or 340 bp upstream of exon 1 containing the 70-bp deletion as shown in Fig. 3A. Vero cells were stimulated with IFN-α (10,000 IU/ml) at 24 h after transfection, and at 48 h after transfection luciferase assays were performed. Data are presented as the fold difference of firefly luciferase activity versus the pGL4.10[luc] empty vector control. The data represent triplicates at least three independent transfections.

normal fibroblasts is not impaired, and (ii) analysis of 5′ RACE products generated from Vero cells, as well as IFN-α/βR$^{-/-}$ MEFs, using the G50DblKo virus failed to detect any proximal promoter (E1-E2)- or distal promoter (E0-E1-E2)-initiated transcripts. However, to more directly assess potential residual proximal promoter activity in the absence of a type I IFN response, we cloned both the proximal promoter and the proximal promoter deletion mutant into the pGL4.10Luc reporter plasmid. These reporter constructs were transfected into Vero cells, in the presence and absence of IFN-α treatment. Importantly, the proximal promoter does not appear to be sensitive to the presence of IFN-α (Fig. 13), which is consistent with the results shown in Fig. 5D where pretreatment with IFN-α has no effect on WT MHV68 growth. Furthermore, the proximal promoter deletion mutant exhibited significant lower promoter activity, in both the presence and absence of added IFN-α. Thus, taken together, these results argue against proximal promoter-driven RTA expression accounting for the rescue of G50DblKo virus replication in the absence of type I IFN.

DISCUSSION

Here we demonstrate that MHV68 gene 50 transcription is more complex than previously reported (6, 12, 16). Based on the current analyses, MHV68 RTA expression can be driven from four distinct promoters, and these promoters drive expression of 5 different spliced gene 50 transcripts. The identification of multiple promoters driving expression of a single gene is not a novel concept; there are many human and viral genes whose expression has been shown to be regulated by multiple promoters (38–42). For example, EBV has been shown to use differential splicing and from 2 distinct promoters in the generation of the transcripts encoding the six EBNA gene products (43–47). The use of multiple promot-

ers is often the result of a complex life cycle and/or, particularly in the case of viruses, the infection of multiple cell types. We have shown that alternatively initiated gene 50 transcripts are conserved in MHV68-, KSHV-, and EBV-infected cells, having previously reported the detection of both proximal and distal promoter-initiated gene 50 transcripts (16). In addition, it has been previously shown by others that HVS RTA expression is driven from distinctly initiated transcripts expressed at different times in the viral replication cycle (48). Here we identify 2 additional gene 50 transcription initiation sites; gene 50 transcripts arising from these promoters could be detected in MHV68 infection of a macrophage cell line (RAW 264.7), a nonhuman primate epithelial cell line (Vero), and IFN-α/βR$^{-/-}$ mouse embryonic fibroblasts, indicating that these promoters appear to be widely active during virus replication and not restricted to a particular cell type. However, we have not carried out a detailed analysis of the abundance of specific gene 50 transcript species as a function of cell type or time postinfection, and it is certainly possible that their activities *in vivo* are more restricted. Thus, the current analyses do not rule out the possibility that the identified gene 50 promoters behave differently depending on cell type infected or address the role that each promoter plays in different cell types during the course of infection.

The utility of MHV68 infection of mice is that it provides a tractable small animal model to identify basic aspects of gammaherpesvirus pathogenesis that may be relevant to the human viruses EBV and KSV. Thus, we have begun to explore whether the complex gene 50 transcription observed during MHV68 replication is conserved in the human viruses. Notably, our preliminary characterization of gene 50 transcription during KSHV reactivation from latently infected B cells has identified multiple distinct gene 50 transcription initiation sites, as well as alternative splicing that is very similar to that observed in MHV68-infected cells (data not shown). Further analyses are necessary to fully characterize these novel gene 50 transcripts expressed during KSHV reactivation from B cells, as well as to characterize BRLF1 transcription during EBV infection.

The data presented here are among a limited number of studies (49) showing that type I interferons play an important role in suppressing MHV68 replication in tissue culture. This is strikingly different from the case for WT MHV68, where *in vitro* growth is not affected by the presence of type I interferons. However, it is important to emphasize that *in vivo* type I interferons play a critical role in controlling acute MHV68 replication, as mice lacking the IFN-α/β receptor are highly susceptible to lethal MHV68 infection (27, 28). In addition, it has previously been shown that type I interferons play a role in controlling viral reactivation from latency (27, 50).

The levels of RTA protein were greatly reduced in G50DblKo-infected cells in the presence of a type I IFN response (Fig. 9A and B), and abrogating the ability to respond to type I IFNs by disrupting IFN-α/βR rescued wild-type levels of RTA expression from the G50DblKo mutant virus (Fig. 9C). Since RTA is the first immediate early gene expressed during gammaherpesvirus infection, it directly and indirectly begins the lytic replication cascade by turning on a variety of downstream genes (51–57). Many of these downstream genes are responsible for an anti-type I interferon response, such as Orf45, M2, and Orf54 (58–63). Importantly, the ability of MHV68 to overcome the type I IFN response appears to be not only essential but also immediate. Growth curves where

IFN-α was added prior to infection and during infection (Fig. 5D) demonstrate that the virus is able to overcome a type I IFN-induced antiviral cell environment; wild-type MHV68, even at a low MOI, is unaffected by IFN-α treatment. We hypothesize, then, that this may involve three distinct mechanisms. First, the virion contains a viral protein(s) able to suppress the type I IFN response. MHV68 proteins associated with the virion have been identified, and this includes the Orf45-encoded protein, which has already been implicated in regulating the type I IFN response (64). Second, RTA may itself be involved in mediating an anti-type I IFN response, but this would likely require that sufficient levels of RTA be expressed in an appropriate time frame postinfection to be effective. Third, RTA expression and function may be insensitive to type I interferon effects and thus able to initiate downstream gene signaling despite the presence of an antiviral cellular state. Future studies will need to address these possibilities.

It is notable that replication of G50DblKo is partially rescued in high-MOI infection. However, replication following high-MOI infection is still severely impaired (as shown in Fig. 6, titers never rise significantly above the input levels). Furthermore, this likely reflects the difference between a single cycle of replication versus the multiple rounds of replication required followed low-MOI infection. Indeed, following high-MOI infection, initial RTA levels following infection with the G50DblKo virus are higher than those in WT virus-infected fibroblasts, but these levels decrease over time (Fig. 6B, hours 16, 20, and 24). This indicates that RTA expression is dysregulated in G50DblKo infected cells and this likely impacts the tightly regulated lytic cascade ultimately leading to diminished virus production and the observed small plaque phenotype (Fig. 6C).

Overall these studies further reveal the complex nature of gammaherpesviruses replication. The identification of 3 additional Orf50 transcripts was surprising but likely illustrates how the virus has evolved to carefully control expression of the essential lytic switch gene. Though beyond the scope of this study, future work will investigate the function of these alternative gene 50 promoters and transcripts, as well as their presence/absence in other gammaherpesviruses. It is clear that in the absence of type I interferons, the newly identified gene 50 transcripts are able to drive viral replication nearly as efficiently as wild-type MHV68. This suggests that these promoters may play a cell type-specific and/or time-dependent role in the viral life cycle. Indeed, independent studies have recently revealed that the N4/N5 promoter is responsive to interleukin-4 (IL-4) treatment in macrophages, which has been shown to trigger MHV68 reactivation from latently infected macrophages (T. A. Reese et al., unpublished data). Another possibility is that upstream-initiated gene 50 transcription may, under some conditions, serve to suppress RTA expression by interfering with transcription from the more proximal gene 50 promoters. Transcriptional interference has been shown before for some EBV transcripts (44, 65–67). In addition, the role of the short ATG-initiated open reading frames in the 5′ untranslated regions of upstream-initiated gene 50 transcripts remains to be investigated.

In summary, the analysis of the G50DblKo mutant extends our understanding of RTA expression and has revealed a hitherto-unappreciated complexity of gene 50 transcription. It is notable that until the analysis of the G50DblKo mutant, little or no impact of type I interferons on wild-type MHV68 replication was observed. This was in stark contrast to the analysis of MHV68 replication during the acute stages of infection in IFN-α/βR$^{-/-}$ mice,

where substantially higher levels of virus replication are observed in the lungs of type I interferon-unresponsive mice than in those of wild-type mice following i.n. virus inoculation (e.g., see Fig. 11) (28). Based on the observations with G50DblKo mutant replication in vitro, it is perhaps reasonable to speculate that during acute virus replication there may be a role for type I IFN-sensitive gene 50 transcription. Future studies will address whether any of the newly identified gene 50 transcripts play such a role during acute virus replication in vivo.

ACKNOWLEDGMENTS

REFERENCES

1. **Young LS, Rickinson AB.** 2004. Epstein-Barr virus: 40 years on. Nat. Rev. Cancer **4:**757–768. http://dx.doi.org/10.1038/nrc1452.
2. **da Silva SR, de Oliveira DE.** 2011. HIV, EBV and KSHV: viral cooperation in the pathogenesis of human malignancies. Cancer Lett. **305:**175–185. http://dx.doi.org/10.1016/j.canlet.2011.02.007.
3. **D'Antonio A, Boscaino A, Addesso M, Piris MA, Nappi O.** 2007. KSHV- and EBV-associated germinotropic lymphoproliferative disorder: a rare lymphoproliferative disease of HIV patient with plasmablastic morphology, indolent course and favourable response to therapy. Leuk. Lymphoma **48:**1444–1447. http://dx.doi.org/10.1080/10428190701387039.
4. **Pyakurel P, Pak F, Mwakigonja AR, Kaaya E, Biberfeld P.** 2007. KSHV/HHV-8 and HIV infection in Kaposi's sarcoma development. Infect. Agents Cancer **2:**4. http://dx.doi.org/10.1186/1750-9378-2-4.
5. **Speck SH, Virgin HW.** 1999. Host and viral genetics of chronic infection: a mouse model of gamma-herpesvirus pathogenesis. Curr. Opin. Microbiol. **2:**403–409. http://dx.doi.org/10.1016/S1369-5274(99)80071-X.
6. **Virgin HW, IV, Latreille P, Wamsley P, Hallsworth K, Weck KE, Dal Canto AJ, Speck SH.** 1997. Complete sequence and genomic analysis of murine gammaherpesvirus 68. J. Virol. **71:**5894–5904.
7. **Barton E, Mandal P, Speck SH.** 2011. Pathogenesis and host control of gammaherpesviruses: lessons from the mouse. Annu. Rev. Immunol. **29:**351–397. http://dx.doi.org/10.1146/annurev-immunol-072710-081639.
8. **Kulkarni AB, Holmes KL, Fredrickson TN, Hartley JW, Morse HC, III.** 1997. Characteristics of a murine gammaherpesvirus infection immunocompromised mice. In Vivo **11:**281–291.
9. **Liang X, Paden CR, Morales FM, Powers RP, Jacob J, Speck SH.** 2011. Murine gamma-herpesvirus immortalization of fetal liver-derived B cells requires both the viral cyclin D homolog and latency-associated nuclear antigen. PLoS Pathog. **7:**e1002220. http://dx.doi.org/10.1371/journal.ppat.1002220.
10. **Ragoczy T, Heston L, Miller G.** 1998. The Epstein-Barr virus Rta protein activates lytic cycle genes and can disrupt latency in B lymphocytes. J. Virol. **72:**7978–7984.
11. **Sun R, Lin SF, Gradoville L, Yuan Y, Zhu F, Miller G.** 1998. A viral gene that activates lytic cycle expression of Kaposi's sarcoma-associated herpesvirus. Proc. Natl. Acad. Sci. U. S. A. **95:**10866–10871. http://dx.doi.org/10.1073/pnas.95.18.10866.
12. **Liu S, Pavlova IV, Virgin HW, IV, Speck SH.** 2000. Characterization of gammaherpesvirus 68 gene 50 transcription. J. Virol. **74:**2029–2037. http://dx.doi.org/10.1128/JVI.74.4.2029-2037.2000.
13. **Pavlova I, Yulin C, Speck S.** 2005. Murine gammaherpesvirus 68 Rta-dependent activation of the gene 57 promoter. Virology **333:**169–179. http://dx.doi.org/10.1016/j.virol.2004.12.021.
14. **Allen RD, DeZalia MN, Speck SH.** 2007. Identification of an Rta responsive promoter involved in driving γHV68 v-cyclin expression during virus replication. Virology **365:**250–259. http://dx.doi.org/10.1016/j.virol.2007.03.021.
15. **Xi X, Persson LM, O'Brien MW, Mohr I, Wilson AC.** 2012. Cooperation between viral interferon regulatory factor 4 and RTA to activate a subset of Kaposi's sarcoma-associated herpesvirus lytic promoters. J. Virol. **86:**1021–1033. http://dx.doi.org/10.1128/JVI.00694-11.
16. **Gray KS, Allen RD, Farrell ML, Forrest JC, Speck SH.** 2009. Alternatively initiated gene 50/RTA transcripts expressed during murine and hu-

man gammaherpesvirus reactivation from latency. J. Virol. **83**:314–328. http://dx.doi.org/10.1128/JVI.01444-08.

17. **Paden CR, Forrest JC, Tibbetts SA, Speck SH.** 2012. Unbiased mutagenesis of MHV68 LANA reveals a DNA-binding domain required for LANA function in vitro and in vivo. PLoS Pathog. **8**:e1002906. http://dx.doi.org/10.1371/journal.ppat.1002906.

18. **Warming S.** 2005. Simple and highly efficient BAC recombineering using galK selection. Nucleic Acids Res. **33**:e36–e36. http://dx.doi.org/10.1093/nar/gni035.

19. **Collins CM, Boss JM, Speck SH.** 2009. Identification of infected B-cell populations by using a recombinant murine gammaherpesvirus 68 expressing a fluorescent protein. J. Virol. **83**:6484–6493. http://dx.doi.org/10.1128/JVI.00297-09.

20. **Weck KE, Barkon ML, Yoo LI, Speck SH, Virgin HI.** 1996. Mature B cells are required for acute splenic infection, but not for establishment of latency, by murine gammaherpesvirus 68. J. Virol. **70**:6775–6780.

21. **Weck KE, Kim SS, Virgin HI, Speck SH.** 1999. B cells regulate murine gammaherpesvirus 68 latency. J. Virol. **73**:4651–4661.

22. **Dong X, He Z, Durakoglugil D, Arneson L, Shen Y, Feng P.** 2012. Murine gammaherpesvirus 68 evades host cytokine production via replication transactivator-induced RelA degradation. J. Virol. **86**:1930–1941. http://dx.doi.org/10.1128/JVI.06127-11.

23. **Pavlova IV, Virgin HW, Speck SH.** 2003. Disruption of gammaherpesvirus 68 gene 50 demonstrates that Rta is essential for virus replication. J. Virol. **77**:5731–5739. http://dx.doi.org/10.1128/JVI.77.10.5731-5739.2003.

24. **Moorman NJ, Willer DO, Speck SH.** 2003. The gammaherpesvirus 68 latency-associated nuclear antigen homolog is critical for the establishment of splenic latency. J. Virol. **77**:10295–10303. http://dx.doi.org/10.1128/JVI.77.19.10295-10303.2003.

25. **Adler H, Messerle M, Koszinowski UH.** 2001. Virus reconstituted from infectious bacterial artificial chromosome (BAC)-cloned murine gammaherpesvirus 68 acquires wild-type properties in vivo only after excision of BAC vector sequences. J. Virol. **75**:5692–5696. http://dx.doi.org/10.1128/JVI.75.12.5692-5696.2001.

26. **Arico E, Robertson KA, Belardelli F, Ferrantini M, Nash AA.** 2004. Vaccination with inactivated murine gammaherpesvirus 68 strongly limits viral replication and latency and protects type I IFN receptor knockout mice from a lethal infection. Vaccine **22**:1433–1440. http://dx.doi.org/10.1016/j.vaccine.2003.10.015.

27. **Barton ES, Lutzke ML, Rochford R, Virgin HW, IV.** 2005. Alpha/beta interferons regulate murine gammaherpesvirus latent gene expression and reactivation from latency. J. Virol. **79**:14149–14160. http://dx.doi.org/10.1128/JVI.79.22.14149-14160.2005.

28. **Dutia BM, Allen DJ, Dyson H, Nash AA.** 1999. Type I interferons and IRF-1 play a critical role in the control of a gammaherpesvirus infection. Virology **261**:173–179. http://dx.doi.org/10.1006/viro.1999.9834.

29. **El-Guindy A, Ghiassi-Nejad M, Golden S, Delecluse HJ, Miller G.** 2013. Essential role of Rta in lytic DNA replication of Epstein-Barr virus. J. Virol. **87**:208–223. http://dx.doi.org/10.1128/JVI.01995-12.

30. **Guito J, Lukac DM.** 2012. KSHV Rta promoter specification and viral reactivation. Front. Microbiol. **3**:30. http://dx.doi.org/10.3389/fmicb.2012.00030.

31. **Wang Y, Tang Q, Maul GG, Yuan Y.** 2006. Kaposi's sarcoma-associated herpesvirus ori-Lyt-dependent DNA replication: dual role of replication and transcription activator. J. Virol. **80**:12171–12186. http://dx.doi.org/10.1128/JVI.00990-06.

32. **Wu TT, Tong L, Rickabaugh T, Speck S, Sun R.** 2001. Function of Rta is essential for lytic replication of murine gammaherpesvirus 68. J. Virol. **75**:9262–9273. http://dx.doi.org/10.1128/JVI.75.19.9262-9273.2001.

33. **Goodwin MM, Canny S, Steed A, Virgin HW.** 2010. Murine gammaherpesvirus 68 has evolved gamma interferon and stat1-repressible promoters for the lytic switch gene 50. J. Virol. **84**:3711–3717. http://dx.doi.org/10.1128/JVI.02099-09.

34. **Krug LT, Collins CM, Gargano LM, Speck SH.** 2009. NF-kappaB p50 plays distinct roles in the establishment and control of murine gammaherpesvirus 68 latency. J. Virol. **83**:4732–4748. http://dx.doi.org/10.1128/JVI.00111-09.

35. **Coleman CB, Nealy MS, Tibbetts SA.** 2010. Immature and transitional B cells are latency reservoirs for a gammaherpesvirus. J. Virol. **84**:13045–13052. http://dx.doi.org/10.1128/JVI.01455-10.

36. **Liang X, Collins CM, Mendel JB, Iwakoshi NN, Speck SH.** 2009. Gammaherpesvirus-driven plasma cell differentiation regulates virus reactivation from latently infected B lymphocytes. PLoS Pathog. **5**:e1000677. http://dx.doi.org/10.1371/journal.ppat.1000677.

37. **Paden CR, Forrest JC, Moorman NJ, Speck SH.** 2010. Murine gammaherpesvirus 68 LANA is essential for virus reactivation from splenocytes but not long-term carriage of viral genome. J. Virol. **84**:7214–7224. http://dx.doi.org/10.1128/JVI.00133-10.

38. **Koenigsberger C, Chicca JJ, II, Amoureux MC, Edelman GM, Jones FS.** 2000. Differential regulation by multiple promoters of the gene encoding the neuron-restrictive silencer factor. Proc. Natl. Acad. Sci. U. S. A. **97**:2291–2296. http://dx.doi.org/10.1073/pnas.050578797.

39. **Delaloy C, Lu J, Houot AM, Disse-Nicodeme S, Gasc JM, Corvol P, Jeunemaitre X.** 2003. Multiple promoters in the WNK1 gene: one controls expression of a kidney-specific kinase-defective isoform. Mol. Cell. Biol. **23**:9208–9221. http://dx.doi.org/10.1128/MCB.23.24.9208-9221.2003.

40. **Ozbun MA, Meyers C.** 1998. Temporal usage of multiple promoters during the life cycle of human papillomavirus type 31b. J. Virol. **72**:2715–2722.

41. **Mitsui S, Nakamura T, Okui A, Kominami K, Uemura H, Yamaguchi N.** 2006. Multiple promoters regulate tissue-specific alternative splicing of the human kallikrein gene, KLK11/hippostasin. FEBS J. **273**:3678–3686. http://dx.doi.org/10.1111/j.1742-4658.2006.05372.x.

42. **Kim JD, Kim CH, Kwon BS.** 2011. Regulation of mouse 4-1BB expression: multiple promoter usages and a splice variant. Mol. Cells **31**:141–149. http://dx.doi.org/10.1007/s10059-011-0018-6.

43. **Bodescot M, Perricaudet M, Farrell PJ.** 1987. A promoter for the highly spliced EBNA family of RNAs of Epstein-Barr virus. J. Virol. **61**:3424–3430.

44. **Woisetschlaeger M, Strominger JL, Speck SH.** 1989. Mutually exclusive use of viral promoters in Epstein-Barr virus latently infected lymphocytes. Proc. Natl. Acad. Sci. U. S. A. **86**:6498–6502. http://dx.doi.org/10.1073/pnas.86.17.6498.

45. **Rogers RP, Woisetschlaeger M, Speck SH.** 1990. Alternative splicing dictates translational start in Epstein-Barr virus transcripts. The EMBO journal. **9**:2273–2277.

46. **Speck SH, Strominger JL.** 1985. Analysis of the transcript encoding the latent Epstein-Barr virus nuclear antigen I: a potentially polycistronic message generated by long-range splicing of several exons. Proc. Natl. Acad. Sci. U. S. A. **82**:8305–8309. http://dx.doi.org/10.1073/pnas.82.24.8305.

47. **Speck SH, Pfitzner A, Strominger JL.** 1986. An Epstein-Barr virus transcript from a latently infected, growth-transformed B-cell line encodes a highly repetitive polypeptide. Proc. Natl. Acad. Sci. U. S. A. **83**:9298–9302. http://dx.doi.org/10.1073/pnas.83.24.9298.

48. **Whitehouse A, Carr IM, Griffiths JC, Meredith DM.** 1997. The herpesvirus saimiri ORF50 gene, encoding a transcriptional activator homologous to the Epstein-Barr virus R protein, is transcribed from two distinct promoters of different temporal phases. J. Virol. **71**:2550–2554.

49. **Wood BM, Mboko WP, Mounce BC, Tarakanova VL.** 2013. Mouse gammaherpesvirus-68 infection acts as a rheostat to set the level of type I interferon signaling in primary macrophages. Virology **443**:123–133. http://dx.doi.org/10.1016/j.virol.2013.04.036.

50. **Mandal P, Krueger BE, Oldenburg D, Andry KA, Beard RS, White DW, Barton ES.** 2011. A gammaherpesvirus cooperates with interferon-alpha/beta-induced IRF2 to halt viral replication, control reactivation, and minimize host lethality. PLoS Pathog. **7**:e1002371. http://dx.doi.org/10.1371/journal.ppat.1002371.

51. **Chen J, Ye F, Xie J, Kuhne K, Gao SJ.** 2009. Genome-wide identification of binding sites for Kaposi's sarcoma-associated herpesvirus lytic switch protein, RTA. Virology. **386**:290–302. http://dx.doi.org/10.1016/j.virol.2009.01.031.

52. **Liu Y, Cao Y, Liang D, Gao Y, Xia T, Robertson ES, Lan K.** 2008. Kaposi's sarcoma-associated herpesvirus RTA activates the processivity factor ORF59 through interaction with RBP-Jkappa and a cis-acting RTA responsive element. Virology **380**:264–275. http://dx.doi.org/10.1016/j.virol.2008.08.011.

53. **Deng H, Liang Y, Sun R.** 2007. Regulation of KSHV lytic gene expression. Curr. Top. Microbiol. Immunol. **312**:157–183. http://dx.doi.org/10.1007/978-3-540-34344-8_6.

54. **Matsumura S, Fujita Y, Gomez E, Tanese N, Wilson AC.** 2005. Activation of the Kaposi's sarcoma-associated herpesvirus major latency locus by the lytic switch protein RTA (ORF50). J. Virol. **79**:8493–8505. http://dx.doi.org/10.1128/JVI.79.13.8493-8505.2005.

55. **Song MJ, Deng H, Sun R.** 2003. Comparative study of regulation of RTA-responsive genes in Kaposi's sarcoma-associated herpesvirus/

human herpesvirus 8. J. Virol. **77:**9451–9462. http://dx.doi.org/10.1128/JVI.77.17.9451-9462.2003.

56. **Ragoczy T, Miller G.** 1999. Role of the Epstein-Barr virus RTA protein in activation of distinct classes of viral lytic cycle genes. J. Virol. **73:**9858–9866.

57. **Chang Y, Lee HH, Chang SS, Hsu TY, Wang PW, Chang YS, Takada K, Tsai CH.** 2004. Induction of Epstein-Barr virus latent membrane protein 1 by a lytic transactivator Rta. J. Virol. **78:**13028–13036. http://dx.doi.org/10.1128/JVI.78.23.13028-13036.2004.

58. **Zhu FX, Sathish N, Yuan Y.** 2010. Antagonism of host antiviral responses by Kaposi's sarcoma-associated herpesvirus tegument protein ORF45. PLoS One **5:**e10573. http://dx.doi.org/10.1371/journal.pone.0010573.

59. **Liang X, Shin YC, Means RE, Jung JU.** 2004. Inhibition of interferon-mediated antiviral activity by murine gammaherpesvirus 68 latency-associated M2 protein. J. Virol. **78:**12416–12427. http://dx.doi.org/10.1128/JVI.78.22.12416-12427.2004.

60. **Liang Q, Fu B, Wu F, Li X, Yuan Y, Zhu F.** 2012. ORF45 of Kaposi's sarcoma-associated herpesvirus inhibits phosphorylation of interferon regulatory factor 7 by IKKepsilon and TBK1 as an alternative substrate. J. Virol. **86:**10162–10172. http://dx.doi.org/10.1128/JVI.05224-11.

61. **Sathish N, Zhu FX, Golub EE, Liang Q, Yuan Y.** 2011. Mechanisms of autoinhibition of IRF-7 and a probable model for inactivation of IRF-7 by Kaposi's sarcoma-associated herpesvirus protein ORF45. J. Biol. Chem. **286:**746–756. http://dx.doi.org/10.1074/jbc.M110.150920.

62. **Zhu FX, King SM, Smith EJ, Levy DE, Yuan Y.** 2002. A Kaposi's sarcoma-associated herpesviral protein inhibits virus-mediated induction of type I interferon by blocking IRF-7 phosphorylation and nuclear accumulation. Proc. Natl. Acad. Sci. U. S. A. **99:**5573–5578. http://dx.doi.org/10.1073/pnas.082420599.

63. **Leang RS, Wu TT, Hwang S, Liang LT, Tong L, Truong JT, Sun R.** 2011. The anti-interferon activity of conserved viral dUTPase ORF54 is essential for an effective MHV-68 infection. PLoS Pathog. **7:**e1002292. http://dx.doi.org/10.1371/journal.ppat.1002292.

64. **Bortz E, Whitelegge JP, Jia Q, Zhou ZH, Stewart JP, Wu TT, Sun R.** 2003. Identification of proteins associated with murine gammaherpesvirus 68 virions. J. Virol. **77:**13425–13432. http://dx.doi.org/10.1128/JVI.77.24.13425-13432.2003.

65. **Paulson EJ, Fingeroth JD, Yates JL, Speck SH.** 2002. Methylation of the EBV genome and establishment of restricted latency in low-passage EBV-infected 293 epithelial cells. Virology **299:**109–121. http://dx.doi.org/10.1006/viro.2002.1457.

66. **Schaefer BC, Strominger JL, Speck SH.** 1997. Host-cell-determined methylation of specific Epstein-Barr virus promoters regulates the choice between distinct viral latency programs. Mol. Cell. Biol. **17:**364–377.

67. **Woisetschlaeger M, Yandava CN, Furmanski LA, Strominger JL, Speck SH.** 1990. Promoter switching in Epstein-Barr virus during the initial stages of infection of B lymphocytes. Proc. Natl. Acad. Sci. U. S. A. **87:**1725–1729. http://dx.doi.org/10.1073/pnas.87.5.1725.